Exploring Ore Grindability Tests with the Steel Wheel Abrasion Test (SWAT) Machine

David Hewitt

Department of Mining and Materials Engineering

McGill University, Montreal

October 2009

A thesis submitted to McGill University in partial fulfillment of the requirements of the degree of Master of Engineering.

ABSTRACT

Steel media wear has been well studied and quantified; one method of quantification is the Comminution Dynamics Lab's Total Media Wear model. It combines simulations, abrasion and corrosion experimental trials to determine wear for the components of milling and grinding ores and minerals for the mining industry. Breakage is an important measure of process efficiency, the greater the number of breakage events per unit energy consumed, the greater the throughput and production. The classic breakage parameter, the Bond Work Index generates an energy term used by mill operators to determine this performance criterion. It has been suggested that the abrasion test, used in the Total Media Wear Model, would be a suitable alternative to the labour and time-consuming Bond Locked-cycle Test. Extensive tests were performed in order to ascertain the possibility of obtaining these two desired results from a single two-minute test. Different steel media samples were tested at different energy levels, and finally by testing under wet and dry conditions. Dry and wet testing did not generate the same wear results. Wear and breakage rates were higher under wet conditions. In general, the size distribution of the abrasive feed evolved into a product with a finer size distribution. Statistical analysis of the data obtained suggests that there is indeed a linear relationship between the energy input into the system and the resultant Work Index value. These results support the suggestion that this test will be able to recreate the Bond Work Indices for minerals; however, more work is required in order to build a working database and determine appropriate correlation factors.

RÉSUMÉ

L'usure des composants ferriques dans les procédés minéralurgiques et un sujet bien étudié. Le laboratoire « Comminution Dynamics » a McGill à crée un modèle nommé « Total Media Wear Model » pour prédire le temps de l'avance nécessaire avant lequel il faudra remplacer les blindages et boulettes. Cette modèle comprend des simulations informatiques et des tests de laboratoire. Une autre mesure utilisée par les contremaitres et operateurs c'est le « Bond Work Index ». L'index donne une valeur approximative pour prédire la consommation d'énergie des moulins. Un test du style « Bond » exige beaucoup d'effort, et temps. Récemment, il a été suggérer qu'on pouvait obtenir des valeurs pour le « Bond Work Index » en utilisant un procédé modifié pour un des tests du « Total Media Wear Model ». Différentes nuances d'acier on été testé avec des niveaux d'énergie variées et sous des conditions sec et humide. Les résultats on démontré que les tests sec/humides n'était pas nécessairement équivalent, de plus, un changement dans la distribution granulométrique s'est produit entre la charge et le produit. Et finalement, l'analyse des données suggère qu'il y a une relation entre la valeur calculée de « Work Index » et l'énergie introduit dans la système. Ces résultats confirment les croyances qu'on pourra déterminer la valeur de « Bond Work Index » en même temps que les données du « Total Media Wear Model ». Cependant, il faudra des tests supplémentaires pour plusieurs types de minéraux. Cela pourra crée une base de données avec lequel des facteurs de corrélations pourront être déterminer.

ACKNOWLEDGEMENTS

I would like to take this opportunity to acknowledge the support received in order to undertake this research as part of the Master's program. Professor James Finch for inviting me into his research group, the Department of Mining and Materials for having me on for another two years and most importantly, Professor Peter Radziszewski for his continuous and endless support and guidance, it has been a privilege to be apart of the Rock and Roll Research Group.

I would also like to acknowledge the staff of both the Mining and Materials Engineering and Mechanical Engineering Departments. Ray Langlois, Monique Riendeau and Helen Campbell for their expertise, guidance and use of the excellent facilities up in the Wong Engineering Building was greatly appreciated. And Gary Savard, John Boisvert and Ray Lemay for their assistance, troubleshooting and technical expertise in keeping our laboratory equipment out of repair shops while continuously improving them to meet our exacting requirements. My research may have been possible, but probably not as much fun without you guys, and for that I am truly grateful.

I would like to thank my colleagues in the Rock and Roll Research Group, my lab and officemates and my friends and Laura, you made time pass more effectively and were an excellent substitute for my natural family when hard at work. And finally I would like to thank my family, my late father, Peter, who was unable to see the end-product and my mother and sister, Cynthia and Louise for their endless support, this is for you guys.

TABLE OF CONTENTS

ABSTRACT **1**

RÉSUMÉ **2**

ACKNOWLEDGEMENTS **3**

TABLE OF CONTENTS **4**

LIST OF FIGURES **6**

LIST OF TABLES **8**

LIST OF SYMBOLS AND ABBREVIATIONS **9**

Chapter 1 MOTIVATION AND INTRODUCTION **10**

1.1 Motivation 11
1.2 Introduction 12

Chapter 2 ABRASIVE WEAR **13**

2.1 Introduction 14
2.2 Wear Overview 14
2.3 Abrasive Wear 14
2.4 Quantification of Wear 16
2.5 SWAT Machine 16
2.6 Abrasion Resistance Testing (and Ranking) 20
2.7 The Total Media Wear Model 22
2.8 Conclusion 23

Chapter 3 BOND WORK INDEX **24**

3.1 Introduction 25
3.2 Bond's Third Theory 25
3.3 Limitations 27
3.4 Other Breakage Work 28
3.5 Applying Bond Ore Breakage Methodology to the SWAT 28
3.6 Locked-Cycle Test 32
3.7 Conclusion 35

Chapter 4 METHODOLOGY **36**

4.1 Introduction 37
4.2 Abrasive and Steel Samples 37

4.3 SWAT Machine Settings 37
4.4 SWAT Machine Experimental Procedure 38
4.4.1 SWAT Machine Dry Procedure (SWAT Locked Cycle additional steps italicized) 38
4.4.2 SWAT Machine Wet Procedure 40
4.4.3 SWAT Machine Slurry Procedure 41
4.5 Sieving Procedure 42
4.6 Wet Abrasive Product Handling 43

Chapter 5 RESULTS 44

5.1 Introduction 45
5.2 Total Media Wear Model Data 45
5.3 SWAT Breakage Data 46
5.4 SWAT Locked-cycle Test Data 52

Chapter 6 DISCUSSION 54

6.1 Introduction 55
6.2 Steel Media Samples and Abrasive Breakage 55
6.3 System Energy and Wear Rate 57
6.4 Work Index 62
6.5 Global Dry/Wet Test Observations 64
6.6 Locked Cycle Test 65
6.7 Standard Deviation 66

Chapter 7 CONCLUSIONS AND RECOMMENDATIONS 72

7.1 Introduction 73
7.2 Conclusions 73
7.2.1 Ore Breakage 73
7.2.2 Test Methodology 74
7.2.3 Energy Requirements 74
7.3 Recommendations for Future Work 75

REFERENCES 79

APPENDIX A 81

APPENDIX B 82

APPENDIX C 83

LIST OF FIGURES

FIGURE 2.1: THREE-BODY ABRASIVE WEAR (CHENJE 2007). 15

FIGURE 2.2: A) RWAT APPARATUS USED FOR ASTM G65-04 (MISRA AND FINNIE 1980), ... 17

FIGURE 2.3: SWAT MACHINE. A) WATER BIN, B) ORE BIN, C) SAMPLE HOLDER, ... 18

FIGURE 2.4: STRAIN GAUGE (BINSFELD)..... 19

FIGURE 2.5: PIPE SAMPLE ABRASION PERFORMANCE (HEWITT, ALLARD ET AL.). 21

FIGURE 2.6: WEAR RATE WITH DIFFERENT ABRASIVES AND MATERIALS (HEWITT, ALLARD ET AL.). 21

FIGURE 2.7: PREDICTED WEAR RATE VS. ACTUAL WEAR RATE FOR ORES TESTED (CHENJE, RADZISZEWSKI ET AL. 2009). 23

FIGURE 3.1: CHANGE IN SIZE DISTRIBUTION (RADZISZEWSKI, HEWITT ET AL. 2008). 30

FIGURE 3.2: WEAR VS. OPERATING WORK INDEX (RADZISZEWSKI, HEWITT ET AL. 2008). 31

FIGURE 3.3: FRICTION COEFFICIENT VS. OPERATING WORK INDEX (RADZISZEWSKI, HEWITT ET AL. 2008). . 31

FIGURE 3.4: ABRASIVE SIZE DISTRIBUTION EVOLUTION DURING LOCKED CYCLE TEST. 32

FIGURE 3.5: W_i EVOLUTION OVER LOCKED-CYCLE TEST. 33

FIGURE 3.6: μ EVOLUTION OVER LOCKED-CYCLE TEST. 34

FIGURE 3.7: ORE BYPASS AROUND THE ABRASION ZONE (RADZISZEWSKI, HEWITT ET AL. 2008) 34

FIGURE 5.1: STEEL MEDIA MASS LOSS AS A FUNCTION OF APPLIED FORCE. 45

FIGURE 5.2: COEFFICIENT OF FRICTION AS A FUNCTION OF APPLIED FORCE. 46

FIGURE 5.3: PRODUCT SIZE DISTRIBUTION AT 155 RPM AND F_{APP}: 250 N. 47

FIGURE 5.4: PRODUCT SIZE DISTRIBUTION AT 155 RPM AND F_{APP}: 500N. 47

FIGURE 5.5: PRODUCT SIZE DISTRIBUTION AT 180 RPM AND F_{APP} 250N. 48

FIGURE 5.6: PRODUCT SIZE DISTRIBUTION AT 180 RPM AND F_{APP}: 500N. 48

FIGURE 5.7: PRODUCT SIZE DISTRIBUTION AT 195 RPM AND F_{APP} 250N. 49

FIGURE 5.8: PRODUCT SIZE DISTRIBUTION AT 195 RPM AND F_{APP} 500N. 49

FIGURE 5.9: STEEL MEDIA SAMPLE WEAR RATE AS A FUNCTION OF ABRASION WHEEL ROTATIONAL SPEED. 50

FIGURE 5.10: STEEL MEDIA SAMPLE WEAR RATE AS A FUNCTION OF APPLIED FORCE. 50

FIGURE 5.11: STEEL MEDIA SAMPLE WEAR AS A FUNCTION OF SPECIFIC ENERGY CONSUMED. 51

FIGURE 5.12: ABRASIVE W_i AS A FUNCTION OF SPECIFIC ENERGY CONSUMED. 51

FIGURE 5.13: LOCKED-CYCLE TEST SIZE DISTRIBUTIONS. 52

FIGURE 5.14: W_i EVOLUTION OVER LOCKED-CYCLE TESTS. 53

FIGURE 5.15: μ EVOLUTION OVER LOCKED-CYCLE TESTS. 53

FIGURE 6.1: WET ABRASION TEST RESULTS FOR 1018 STEEL(CHENJE 2007). 55

FIGURE 6.2: STEEL MEDIA WEAR RATE AS A FUNCTION OF SPECIFIC ENERGY FOR 1018 STEEL. 58

FIGURE 6.3: STEEL MEDIA WEAR AS A FUNCTION OF SPECIFIC ENERGY FOR 4140 STEEL. 59

FIGURE 6.4: LINE OF BEST FIT REGRESSION ANALYSIS FOR 1018 STEEL SAMPLES, DRY ONLY. 60

FIGURE 6.5: LINE OF BEST FIT REGRESSION ANALYSIS FOR 1018 STEEL SAMPLES, WET ONLY. 60

FIGURE 6.6: LINE OF BEST FIT REGRESSION ANALYSIS FOR 4140 STEEL SAMPLES, DRY ONLY. 61

FIGURE 6.7: LINE OF BEST FIT REGRESSION ANALYSIS FOR 4140 STEEL SAMPLES, WET ONLY. 61

FIGURE 6.8: LINEAR RELATIONSHIP DEMONSTRATED FOR WORK INDEX AS A FUNCTION OF SPECIFIC ENERGY. 63

FIGURE 7.1: FINES, A), TRAPPED IN WHEEL BRUSH, B), FROM TRADITIONAL WET TESTING. 76

FIGURE 7.2: NEW WATER FLUSHING SYSTEM USED FOR WET TESTS. 77

LIST OF TABLES

TABLE 6-1: REGRESSION ANALYSIS PERFORMED FOR 1018 AND 4140 STEEL MEDIA TESTS BY MINITAB 15. 62

TABLE 6-2: REGRESSION ANALYSIS FOR FIGURE 5.12 (FIGURE 6.8). 63

TABLE 6-3: RELATIVE STANDARD DEVIATION OF SAMPLE MASS LOSS VALUES FOR 1018 DRY AND WET TESTS RESPECTIVELY. 67

TABLE 6-4: RELATIVE STANDARD DEVIATION OF SAMPLE MASS LOSS VALUES FOR 4140 DRY AND WET TESTS RESPECTIVELY. 67

TABLE 6-5: RELATIVE STANDARD DEVIATION OF FRICTION COEFFICIENT VALUES FOR 1018 DRY AND WET TESTS RESPECTIVELY. 67

TABLE 6-6: RELATIVE STANDARD DEVIATION OF FRICTION COEFFICIENT VALUES FOR 4140 DRY AND WET TESTS RESPECTIVELY. 68

TABLE 6-7: RELATIVE STANDARD DEVIATION OF WEAR RATE VALUES FOR 1018 DRY AND WET TESTS RESPECTIVELY. 68

TABLE 6-8: RELATIVE STANDARD DEVIATION OF WEAR RATE VALUES FOR 4140 DRY AND WET TESTS RESPECTIVELY. 68

TABLE 6-9: RELATIVE STANDARD DEVIATION OF WORK INDEX VALUES FOR 1018 DRY AND WET TESTS RESPECTIVELY. 69

TABLE 6-10: RELATIVE STANDARD DEVIATION OF WORK INDEX VALUES FOR 4140 DRY AND WET TESTS RESPECTIVELY. 69

TABLE 6-11: RELATIVE STANDARD DEVIATION OF ENERGY INPUT VALUES FOR 1018 DRY AND WET TESTS RESPECTIVELY. 70

TABLE 6-12: RELATIVE STANDARD DEVIATION OF ENERGY INPUT VALUES FOR 4140 DRY AND WET TESTS RESPECTIVELY. 70

TABLE 6-13: RELATIVE STANDARD DEVIATION OF SPECIFIC ENERGY INPUT VALUES FOR 1018 DRY AND WET TESTS RESPECTIVELY. 71

TABLE 6-14: RELATIVE STANDARD DEVIATION OF SPECIFIC ENERGY INPUT VALUES FOR 4140 DRY AND WET TESTS RESPECTIVELY. 71

LIST OF SYMBOLS AND ABBREVIATIONS

SWAT	Steel Wheel Abrasion Test
RWAT	Rubber Wheel Abrasion Test
HSLA	High Strength Low Alloy
ASTM	American Society for Testing and Materials
AISI	American Iron and Steel Institute
W_i	Bond Work Index
W_{oi}	Bond Operating Work Index
kWhr/T	kilowatt hours per tonne
SAG	Semi-Autogenous Grinding
N	Newtons
RPM	Revolutions per Minute
μ	Friction Coefficient
T	Torque
F_A	Applied Force
r	Abrasion Wheel Radius

Chapter 1 MOTIVATION AND INTRODUCTION

1.1 Motivation

The Comminution Dynamics Laboratory in the Department of Mechanical Engineering at McGill University is dedicated to the better understanding of the breakage process of rocks and ore and how this breakage occurs in existing mining equipment. From there, the optimization of existing mining equipment can be studied and implemented allowing for the efficient use of resources for the energy intensive comminution processes. Work done previously in the lab has resulted in a better understanding of charge motion and better prediction of media wear in tumbling mills. Expanding on the latter, one of the decoupled wear model's tests is aptly suited for studying ore breakage. Thus, allowing for a number of valuable results being extrapolated from a single test.

Combining steel media wear determination with that of the Bond Work Index, operators will be able to understand the power needs of their mills for breakage as well as optimizing their machines for the more efficient use of their resources. Currently this work is being performed in a laboratory in Montreal, QC. The companies in need of these tests are thousands of kilometers from this site; it is the hope of the author that this body of work will, in the future, allow for on-site testing. This machine could easily be used in open pits to determine energy requirements for each of the blocks to be processed, or it could be used on mill circuit feed for quality control, process monitoring, etc.

1.2 Introduction

Abrasive wear plays an important role in the mining industry; it can be a sizeable portion of maintenance budgets. Another major cost for the mining industry is the power consumption of the mill. Efficient size reduction, or breakage, of ore and hard rock for future steps in processing can be a daunting task. When combining these requirements with the need to limit abrasive wear of the machinery, one can see that any relevant assistance would be tremendously valuable.

The goal of this work is to explore the possibility of combining two pre-existing test procedures in order to create a single test that would generate this required information for operators. This will be achieved by:

1. Understanding abrasive wear and how it is to be studied and predicted
2. Investigating how ore breakage can be studied with similar test methodologies.
3. Examining and understanding abrasive wear and breakage under various conditions in an effort to better understand their behavior.
4. Proposing a methodology for concurrently testing abrasive wear and ore breakage.

Chapter 2 ABRASIVE WEAR

2.1 Introduction

The subject of wear will be covered briefly in the following chapter. It will begin with an overview of the phenomenon of wear, how wear is quantified, and its role in mineral processing. Efforts made to better understand and minimize wear will round out the discussion.

2.2 Wear Overview

Wear is an interaction between a surface and its environment. The end result is a quantifiable mass lost from the surface. It can be described in terms of the number of interacting species involved (two-body or three-body are common) and how this interaction occurs (physical, chemical, etc). Three-body abrasive wear will be further elaborated upon in this work; however, many other types of wear exist and are the topic of other research (Chenje 2007) (Radziszewski 2002) (Hawk, Wilson et al. 1999).

2.3 Abrasive Wear

The prevalent form of wear in this research, and economically significant to many industries, (Hawk, Wilson et al. 1999; Radziszewski 2002; Chenje 2007) abrasive wear occurs when forces exerted on particles, harder than the surface they are in contact with, cut into the surface and create grooves or troughs. The surface material displaced by this action is quantified as the mass lost due to abrasive wear. Three-body abrasive wear involves two hard surfaces with an abrasive media forced between them. See Figure 2.1

below. This type of wear is present in abrasive wear testing as performed with the ASTM G-65 apparatus, discussed in greater detail shortly (ASTM 2006).

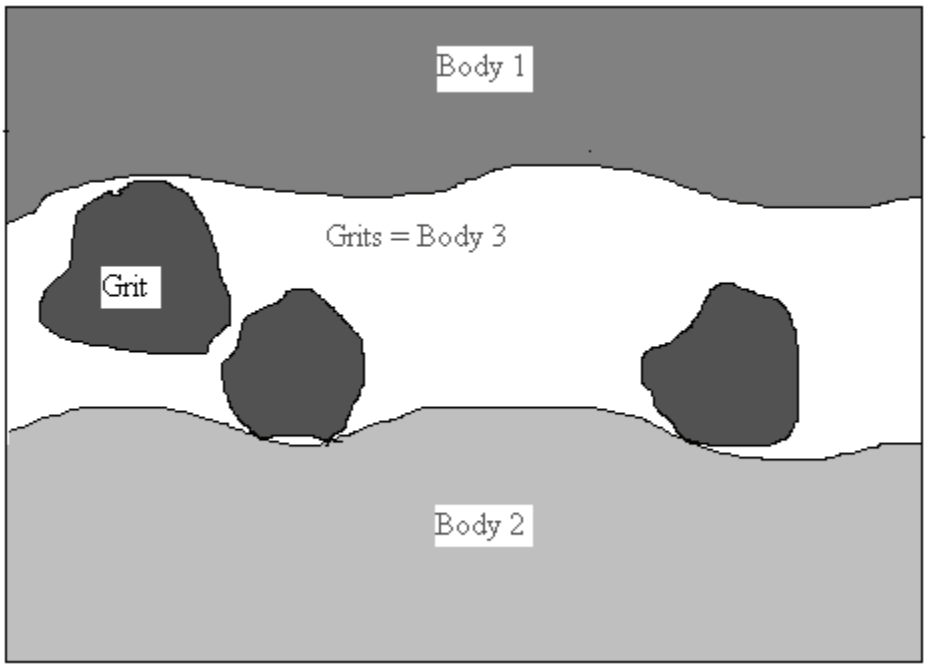

Figure 2.1: Three-body abrasive wear (Chenje 2007).

Depending on the hardness of the surfaces involved and the amount of force applied, one surface should wear preferentially. This wear mechanism is of great importance in mineral processing because of the nature of the processes performed (Radziszewski 2002). Ore, a hard rock, is broken by mechanical means such as crushing and grinding; it is transported by conveyors and chutes or pumped through pipelines. The ore can be harder than the surfaces it contacts throughout these processes, and therefore will abrade, gouge and/or cut these surfaces, no matter the particle size. The replacement of worn parts represents a significant cost to companies (Hawk, Wilson et al. 1999).

2.4 Quantification of Wear

Since it has been established that wear is an issue, it must now be measured and then somehow minimized. Previous work in the laboratory has demonstrated that the modified G-65 test, further referred to as the SWAT, can perform such tasks (Chenje, Radziszewski et al. 2009; Radziszewski 2009). With the use of a strain gauge on the drive shaft, the energy input into the system can be measured. The mass loss of the steel media sample is simply the differential mass readings of the sample before and after performing the test. These two measurements create a value for the media sample's wear rate. This value is used to rank material performance (abrasion resistance), discussed shortly, as well as being part of the total media wear model (Hewitt, Allard et al. ; Chenje 2007).

2.5 SWAT Machine

The test apparatus used for this research is a variation of the apparatus used in the ASTM G65–04 "Standard Test Method for Measuring Abrasion Using the Dry Sand/Rubber Wheel Apparatus," (ASTM 2006), as seen in Figure 2.2A. The RWAT apparatus consists of an abrasive hopper, rubber-lined wheel driven by a 1 hp motor and a sample holder fixed to a lever arm, Figure 2.2B. This lever arm is loaded with weights in order to transmit the required applied force to the sample-wheel interface (ASTM 2006). Differences between the two apparatus' are as follows: The abrasive feed for the standard test is always a standard Ottawa Foundry Sand, while the SWAT can be operated with any abrasive preferably of that size fraction (Hewitt, Allard et al.).

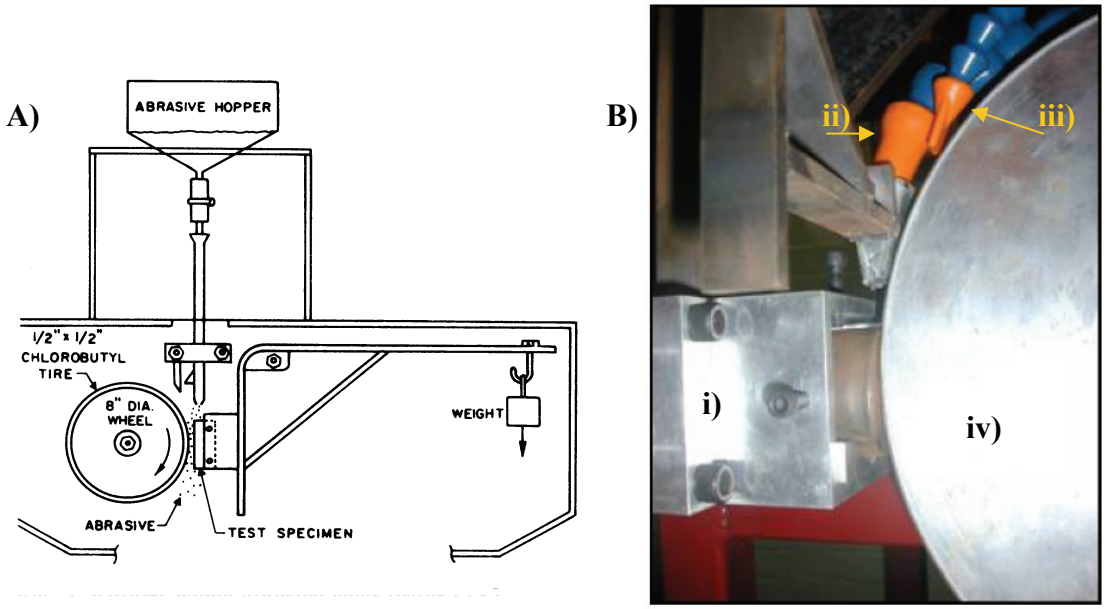

Figure 2.2: A) RWAT apparatus used for ASTM G65-04 (Misra and Finnie 1980), B) i) SWAT steel media sample holder, ii) ore feed, iii) water feed and iv) steel wheel.

The wheel diameter of the standard test is fixed at 228.6 mm (9 inches) while the SWAT typically operates with a wheel diameter of 285.8 mm (11.25 inches). Wheel material also varies, the standard wheel is chlorobutyl rubber-lined steel, while the SWAT is entirely steel. The standard test also has specific operating parameters including: wheel speed, applied force and test time (or lineal abrasion). The SWAT machine has a variable operating speed, determined by the motor control unit, it also has a range of applied forces used for testing. Finally, testing is usually only performed for 2 minutes, but this has been amended as required under certain circumstances. As well, the SWAT machine's drive shaft has been equipped with a strain gauge which is used to calculate the energy input to the system. The SWAT machine can be seen in Figure 2.3 below.

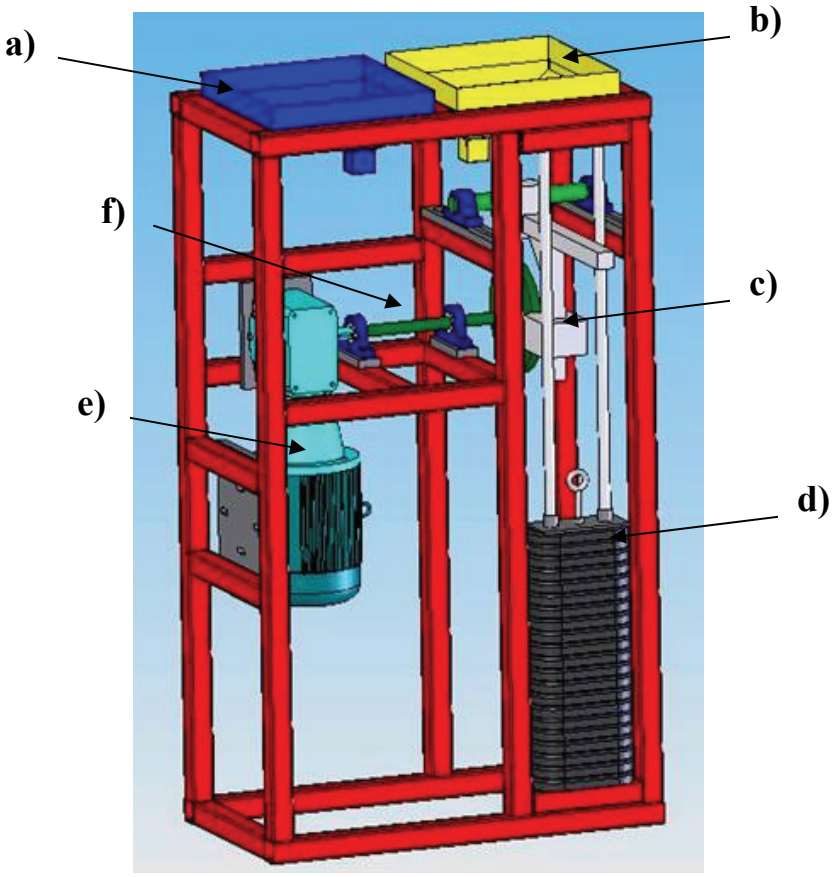

Figure 2.3: SWAT Machine. a) water bin, b) ore bin, c) sample holder, d) weight stack, e) motor and gearbox assembly and f) instrumented drive shaft.

The strain gauge used on the SWAT machine is supplied by Binsfeld Engineering, it is a full bridge strain gauge, meaning that there is only one gauge required for strain and torque measurement. The gauge is precisely bonded to the drive shaft of the SWAT machine, meaning that any strain felt by the shaft will be picked up by the gauge. A DC signal is sent through the strain gauge at all times. In its relaxed state, there is no resistance to this signal; however, as the shaft is strained or torqued, this resistance will vary, see Figure 2.4 below, creating a change in the signal picked up by the receiver. These different signals are then converted into useful information with the use of a computer and calibration or conversion factors.

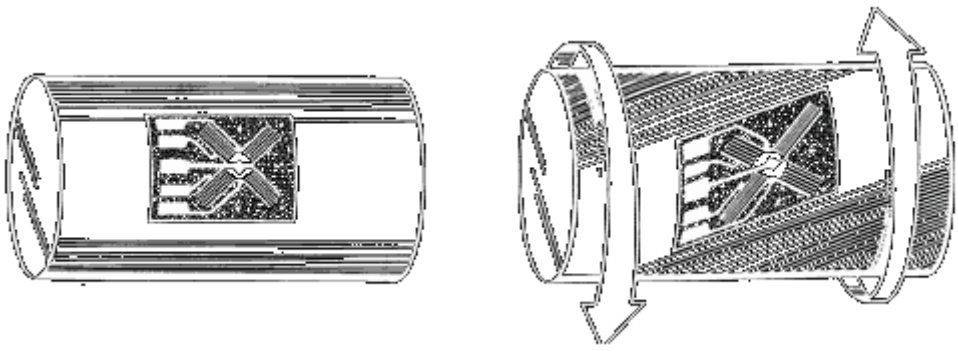

Figure 2.4: Strain gauge (Binsfeld).

The calculated torque value is the average of all toque measurements recorded during the two-minute test period. This value, T (Nm), is used along with the applied force, F_A (N), and the abrasion wheel radius, r (m), in the following equation to determine the friction coefficient μ.

$$\mu = \frac{T}{F_A r} \qquad \textbf{(2-1)}$$

Another interesting value that can be calculated from the strain gauge data is the energy input to the system, in kilowatt hours (kWhr). This allows the operator to calculate abrasive wear rates as well as the potential to study breakage rates for mineral processing.

2.6 Abrasion Resistance Testing (and Ranking)

Work performed in the lab has been used to determine comparative abrasion resistance between pipe lining materials for a paste backfill mining operation in Northern Ontario. The objectives of these tests were to compare the current pipe material with that of new, potential replacement pipe linings. Of the nine competitive samples tested, only one performed worse than the current pipe material. Tests were run with standard Ottawa Foundry Sand, seen in Figure 2.5 below, and, attempts were made to run further tests with the mine tailings as the abrasive. Unfortunately, the size distribution of the tailings fell outside of the typical abrasive size distribution, testing required modified procedures. The modified procedures required the fine tailing particles to be transported in a slurry suspension from the hopper to the test chamber. The slurry mixture was approximately 40% solids by mass. This abrasive tailing slurry was tested on four of the 10 samples. These results are listed in Figure 2.6 below. It is evident that the slurries, both current and proposed tailings, abraded the samples much less than the dry abrasives. This trend appears consistent for all four abrasives tested. This demonstrates the possibility of further expanding testing procedures from dry abrasive testing into the areas of wet testing and slurry testing.

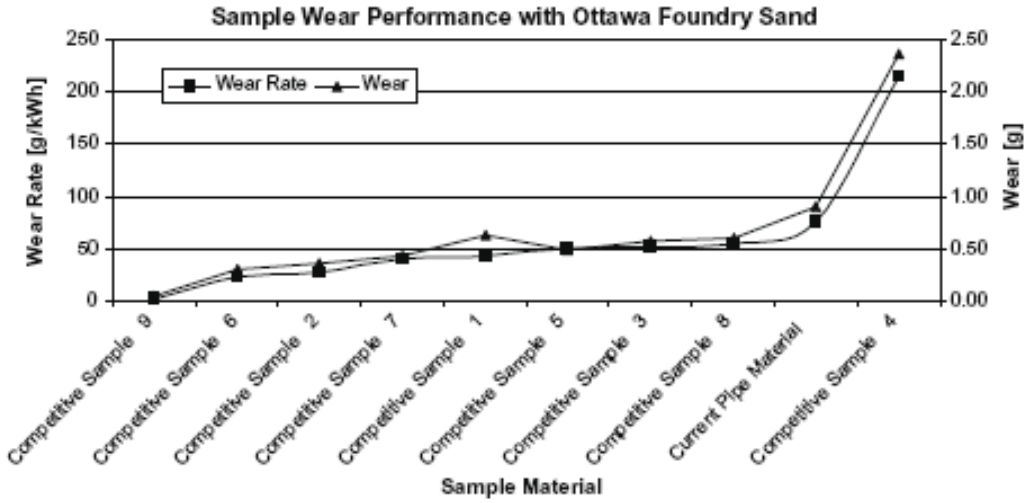

Figure 2.5: Pipe sample abrasion performance (Hewitt, Allard et al.).

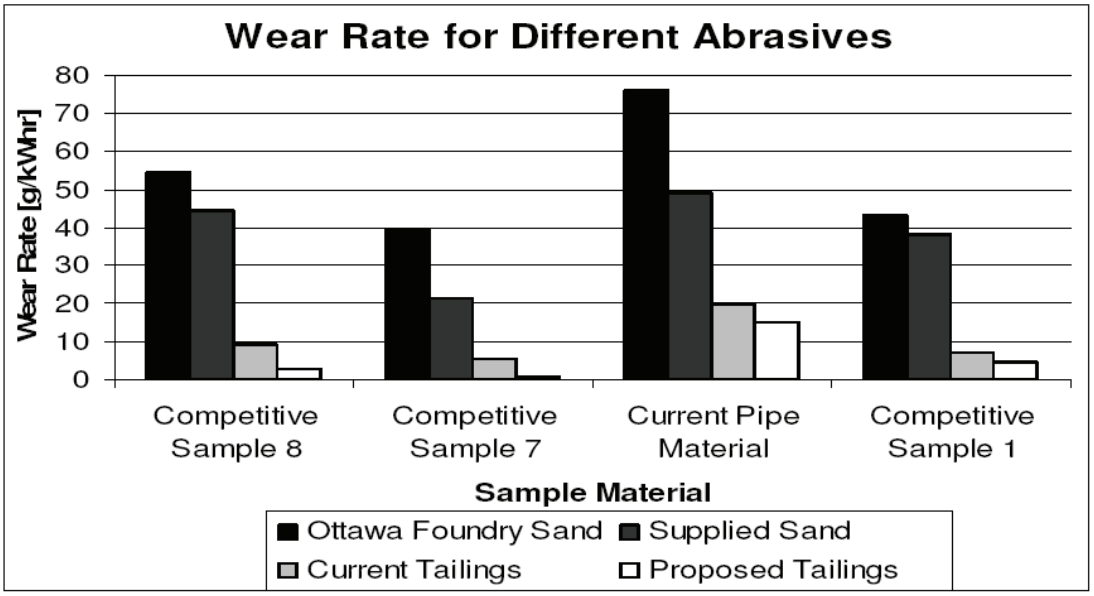

Figure 2.6: Wear rate with different abrasives and materials (Hewitt, Allard et al.).

2.7 The Total Media Wear Model

The Total Media Wear Model is the product of previous research in the Comminution Dynamics Lab (Radziszewski 2002; Chenje and Radziszewski 2004). Simply put; it is the sum of individual wear components present in grinding mills:

$$\dot{m}_{total} = \sum_{i=1}^{3} \dot{m}_i \qquad \textbf{(2-2) (Radziszewski 2002)}$$

where i = 1, 2, 3 corresponding to abrasion, corrosion and impact. Impact was later dropped due to the nature of impact failure (often catastrophic) and the minimal role played overall by impact in tumbling mills (Chenje 2007; Chenje, Radziszewski et al. 2009). The Abrasive Wear Component is as follows:

$$\dot{m}_{abrasion} = k_1 E_{abr} \qquad \textbf{(2-3) (Chenje, Radziszewski et al. 2009)}$$

The abrasion component is the product of the abrasion energy, E_{abr} (J), and the proportionality constant, k_1 (kg/J). The abrasion energy is calculated from DEM simulations while the k_1 value is determined by the SWAT test (Chenje, Radziszewski et al. 2009).

The model was then tested with seven different ores to ascertain its validity. The result of these tests can be seen in Figure 2.7, the x-axis representing the actual wear rate at the mine site, the y-axis representing the predicted wear rate calculated with the Total Media Wear Model.

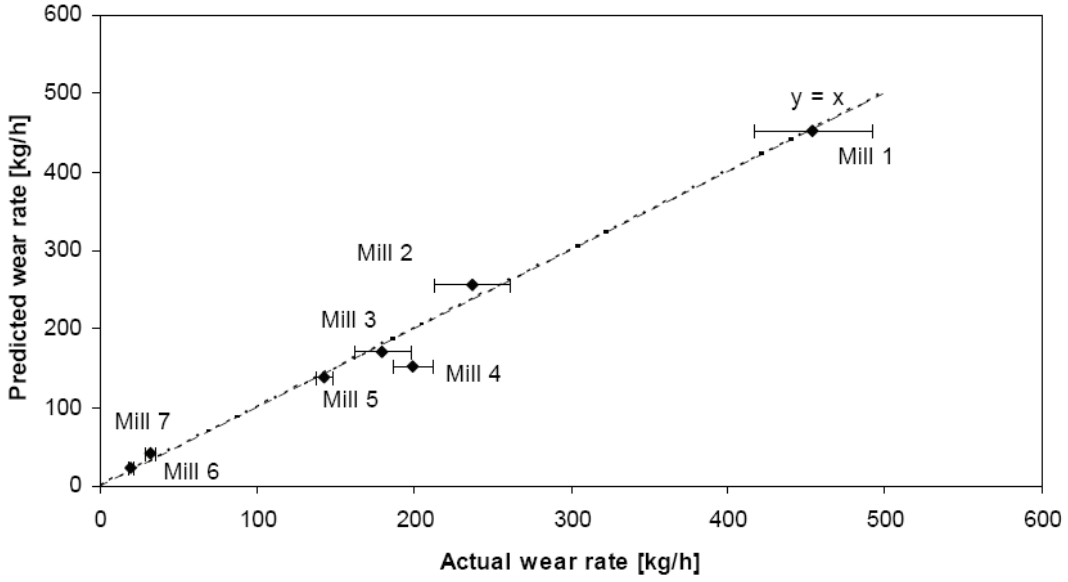

Figure 2.7: Predicted wear rate vs. actual wear rate for ores tested (Chenje, Radziszewski et al. 2009).

Finally, the modeling efficiency was used to determine the goodness of fit for the model. The result is an EF value of 0.96, a perfect fit would be 1.0 (Chenje, Radziszewski et al. 2009).

2.8 Conclusion

Three-body abrasive wear plays a very important role in mineral processing; recreating this wear mode in a laboratory setting has been successfully achieved by adapting the ASTM G65 test apparatus, creating the SWAT machine. This machine is currently used not only to comparatively test metallic samples for their wear resistance, but also for the prediction of steel media wear inside tumbling mills with impressive accuracy. With the value this machine and testing procedure hold, it would be beneficial to examine further uses for this laboratory setup.

Chapter 3 BOND WORK INDEX

3.1 Introduction

The following chapter will describe Bond's work surrounding his Third Theory of Comminution. It will concisely explain its origins, evolution and its modern day purpose in industry. Shortcomings and other breakage models will be briefly examined as well. Finally, having understood the limitations of this test, it will investigate whether an alternative methodology, using the SWAT Machine can be developed.

3.2 Bond's Third Theory

Fred Bond published his Third Theory in 1952, it builds on Rittinger and Kick's theories. Rittinger's stated that the useful work done in crushing and grinding is directly proportional to the new surface area produced, or indirectly proportional to the product's diameter. The Kick theory examined the stress-strain relation of cubes under compression suggesting that the work required is proportional to the volume loss of the feed particles. Bond revisited these theories and built on them, the Third Theory states that the energy required to grind a given ore from an infinite size down to 80% passing 100 μm can be calculated as follows:

$$W_i = W\left(\frac{\sqrt{F}}{\sqrt{F-\sqrt{P}}}\right)\sqrt{\frac{P}{100}} \qquad \textbf{(3-1) (Bond 1952)}$$

where W_i is the Work Index, the work required to reduce an ore to its target product size (kWh/T), W is the actual work input to the system (kWh), F is the size of the feed (μm) and P is the product size (μm). Bond created a database from his work with various ore

and rock samples, along with his test methodology, this can be found in his manuscript (Bond 1952). The test is a locked-cycle test, borne from the finding that batch tests were insufficient for predicting the required work for closed-circuit and multi-mineral milling. There are a minimum number of cycles required to complete the test, usually seven. Above this number, the test has demonstrated itself to be very reliable when used within its stated limitations (Mosher and Tague 2001). Since then, it has been widely used for feasibility studies (Chakrabarti 2000), mill sizing and performance evaluation (Deniz and Ozdag 2003).

The Third Theory takes many forms, such as the equation for the Ore Grindability Test:

$$W_i = 1.1 \frac{44.5}{P_i^{0.23} G^{0.82} \left(\frac{10}{\sqrt{P_{80}}} - \frac{10}{\sqrt{F_{80}}} \right)} \qquad \textbf{(3-2) (Bond 1960)}$$

W_i is again the Work Index (kWh/T), P_i is the closing sieve size (μm), G is the mass of P_i's undersize (or grinding rate) and F_{80} and P_{80} are 80% passing size of the Feed and Product respectively. Once the Work Index is determined, the Operating Work index, W_{oi} can be verified periodically by in-house technical staff in order to evaluate mill performance. This work index, Equation 3, is simply a derivation of Bond's earlier work, it can be readily found in literature.

$$W = 10 W_{oi} \left(\frac{1}{\sqrt{P_{80}}} - \frac{1}{\sqrt{F_{80}}} \right) \qquad \textbf{(3-3)}$$

3.3 Limitations

There are a lot of interesting limitations that have been discovered over the past forty-five years, many people have assumed this relationship would meet all of their needs, and ultimately, they abuse its power with little or no consideration for the Work Index's intended use for the outcomes (Powell and Morrison 2007). It is clearly stated that the outcome of a Bond Grindability Test was intended to deliver the power requirement (kWh/T) for an average 2.4m (8ft) overflow mill in closed circuit (Bond 1960). With comminution circuits increasingly divergent from this one grinding style, applying Bond's methodology is expected to diverge much in the same manner. Modifications have been successfully made when accommodating moderately larger mills, ball sizes and mill operating speeds, but SAG Milling and ultra-fine grinding have proven to be beyond the scope of the Grindability Test as Bond intended (Powell and Morrison 2007).

Other sources of variability in the Bond Test arise from grinding efficiency of machinery, heterogeneity in the ore (Bond 1960), the presence of clay is often detrimental, generating inconsistent results, requiring the constant evaluation through W_{oi} calculations. Also, exploring alternative F and P values can have an impact on the W_i values. Intuitively, more energy is required to grind a given ore to a finer size (Tuzun 2001). In addition, finer material present in the mill can be prohibitive to size reduction (Free, McCarter et al. 2005); their action of coating the liners and media actually absorbs useful energy which detracts from required breakage energy (Menendez-Aguado, Dzioba et al. 2005).

3.4 Other Breakage Work

With all this discussion of limitations to the Bond Test, it is important to note that researchers did in fact seek out alternatives to Bond's Third Theory. These other breakage models, while important to mineral processing, have not completely supplanted the Bond Work Index as the benchmark test. Single Particle Breakage Tests have been used widely with success. Two such tests: the Pendulum Test (Narayanan 1987) and the Drop Weight Test (DWT) have been promoted by the JKMRC. For this particular work, it is sufficient to know that these tests do exist, in part to better predict SAG mill performance, but they too have their limitations (Powell and Morrison 2007). Attempts have been made in the past to correlate Bond and the JK DWT; however, it is typically only possible within a particle size range of 3.0 - 0.7 mm (Menendez-Aguado, Dzioba et al. 2005).

3.5 Applying Bond Ore Breakage Methodology to the SWAT

Having previously discussed abrasive wear testing, it is time to examine the Bond Index and how such a value can be obtained from the SWAT Machine. The requirements are simple: energy put into breaking the ore and the size of the broken ore. The only addition to the current abrasive wear test procedure will involve the sizing of the feed and product material. Using the standard abrasive Ottawa foundry sand that the ASTM G-65 test requires, the operator already possesses the feed size distribution, all that remains is to collect the abrasive that has been run through the machine for sizing. The forces between the steel wheel and the steel media sample will be high enough that the abrasive particles

will be broken as they pass between the two surfaces (Radziszewski 2002; Gates, Gore et al. 2007). Therefore it is reasonable to assume that the portion of the abrasive product size distribution that deviates from the feed size distribution represents the progeny of the particles that passed between the steel wheel and the steel media sample. All other information required has been previously gathered or calculated from the pre-existing test methodology.

Preliminary work has been undertaken to examine the feasibility of applying the Bond breakage methodology to the SWAT machine. This included a small set of tests chosen to ascertain whether this work would in fact generate interesting results. These results were presented at the IMPC Conference in Beijing 2008. From these results, the full battery of tests took shape. At this time, only the IMPC results will be discussed.

The IMPC tests were conducted under the following conditions: one type of steel media sample, one wheel rotational speed, one type of abrasive and three different applied forces. Figure 3.1 shows the initial size distribution of the abrasive. It also shows the evolution of the size distribution after having passed through the SWAT machine. There are a larger percentage of smaller particles present in the product than the feed. This comes at the expense of the larger particles in the size distribution.

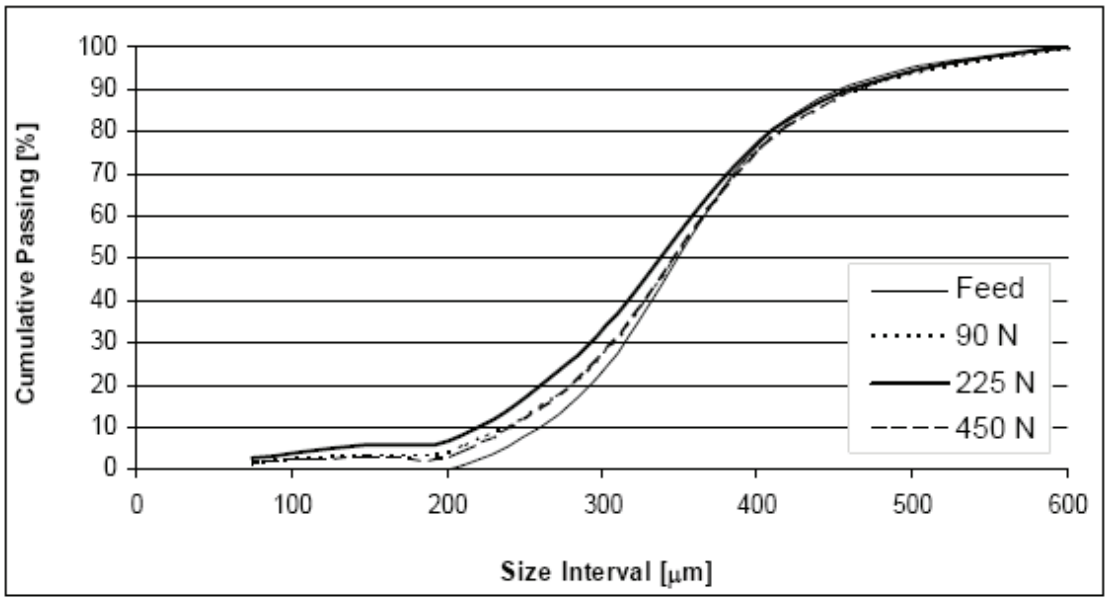

Figure 3.1: Change in size distribution (Radziszewski, Hewitt et al. 2008).

Next, the Operating Work Index, W_{oi}, and wear rate were calculated from the results. Plotting the average results from the three different forces gave the relationship seen below in Figure 3.2. The wear rate will increase with an increasing W_{oi} value. This makes sense; the higher the work index for a given ore, the more energy required per tonne ore processed to achieve the desired result. And the greater the energy put into the system, the greater the energy losses will be (heat, noise, wear etc.). Figure 3.3 demonstrates the relationship between the friction coefficient, μ, and the W_{oi} values.

Figure 3.2: Wear vs. operating work index (Radziszewski, Hewitt et al. 2008).

Figure 3.3: Friction coefficient vs. operating work index (Radziszewski, Hewitt et al. 2008).

3.6 Locked-Cycle Test

After completing the previous tests, a locked-cycle methodology was adapted to the SWAT Machine. That is, after each test, the product broken to sizes below 105 μm was removed and the equivalent mass of fresh feed was added. As mentioned earlier, a minimum of seven grinding cycles must be performed in the traditional Bond Locked-Cycle test. However, only four cycle tests were performed, giving the following results.

First, in Figure 3.4, the size distribution of the abrasive is revisited. It can be seen that it greatly resembles those seen in Figure 3.1 in the sense that after passing through the SWAT, the sand has been broken. More importantly, each subsequent pass after the initial one shows a greater percentage of finer abrasive material being produced.

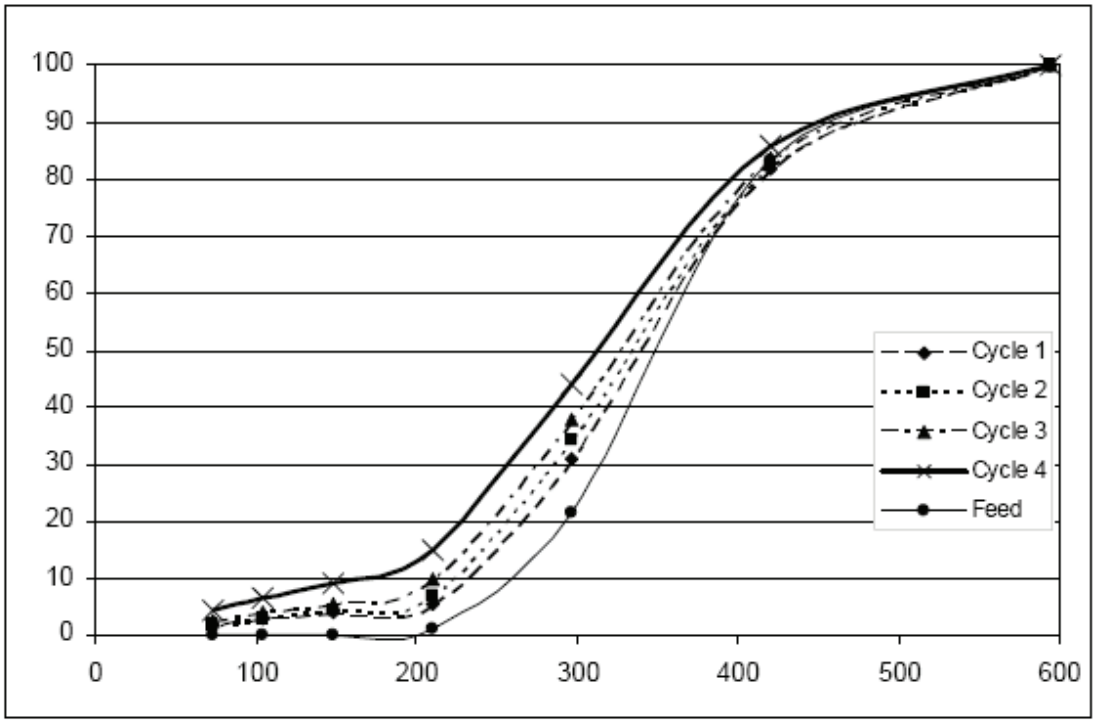

Figure 3.4: Abrasive size distribution evolution during locked cycle test.

Next, when examining the Work Index, W_i, from the different cycles and % Passing the closing size, it was noticed that these values tend to converge the more cycles the abrasive experienced. Also, with the greater number of cycles the abrasive experienced, the friction coefficient decreased. The results are displayed in Figure 3.5 and Figure 3.6 respectively.

In addition to these results, some observations were made concerning this group of tests. As per the ASTM standard, a sand curtain is required such that there is always sand in between the steel media sample and the wheel during a test. This leads to excess sand gathering in the container below. The excess means that sand has bypassed the two steel surfaces and therefore was not subjected to any force whatsoever, and therefore is not broken. A photograph of this phenomenon has been included, see Figure 3.7.

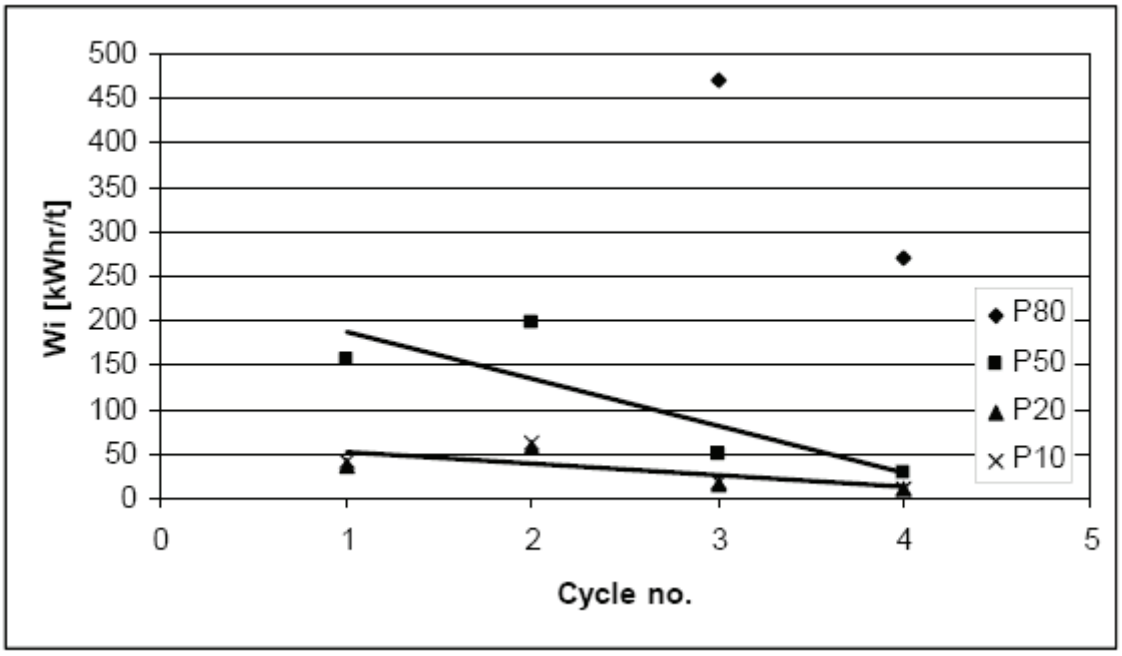

Figure 3.5: W_i evolution over locked-cycle test.

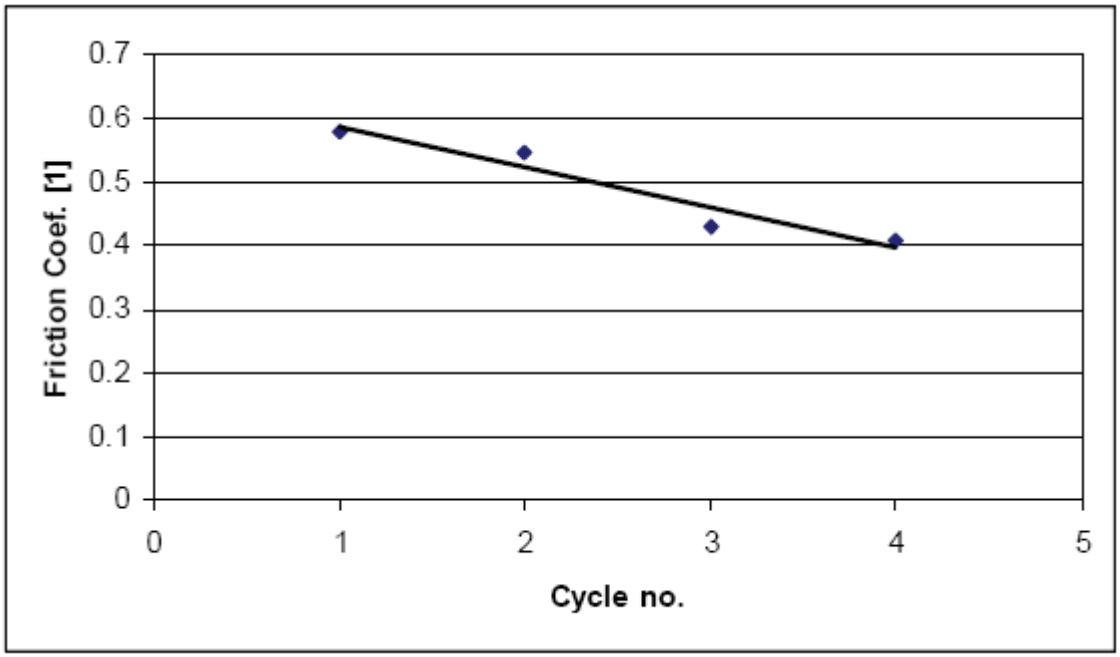

Figure 3.6: μ evolution over locked-cycle test.

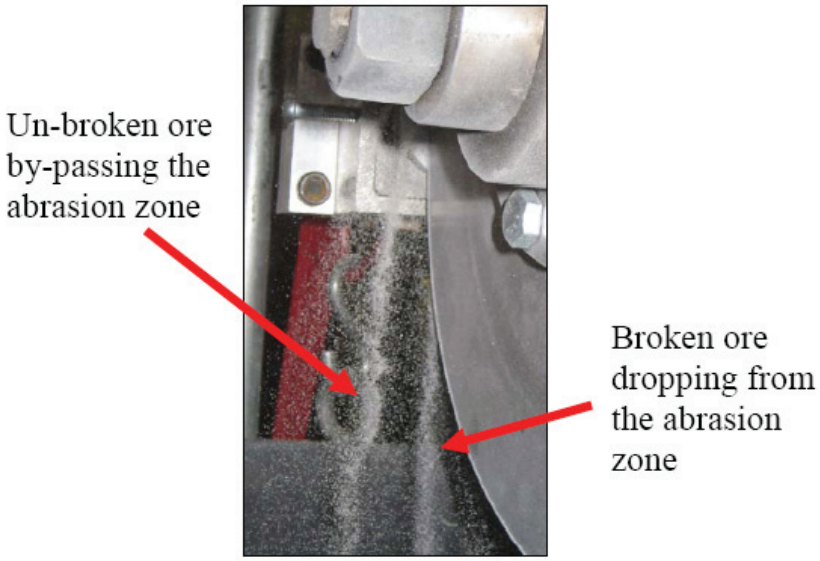

Figure 3.7: Ore bypass around the abrasion zone (Radziszewski, Hewitt et al. 2008)

Now, considering the locked cycle test portion of this work, the four cycles completed in this case represent the use of only 3 kg of abrasive. A complete locked cycle test

performed with the SWAT machine would hypothetically yield the desired results in less than 5 kg. This information would make mill operators and laboratory technicians smile as it significantly limits the negatives associated with the Bond test (Aksani and Sonmez 2000; Deniz and Ozdag 2003).

3.7 Conclusion

Building upon the work of Rittinger and Kick, Bond was able to create the benchmark for the minerals industry to grow from. Many noted limitations have somewhat dated the Bond Grindability Test. Regardless of this fact, it remains a cornerstone of mineral processing equipment sizing, feasibility studies and ongoing plant performance evaluation regardless of the introduction of newer breakage models. With this staying power, it is evident that testing for this value remains interesting to operators. Having uncovered some interesting relationships in the preliminary work, further research will be performed to better understand these relationships and how the SWAT machine test methodology can update and enhance the Bond Grindability Test.

Chapter 4 METHODOLOGY

4.1 Introduction

This section will demonstrate how such an objective will be achieved. The tests will examine the breakage of Ottawa Foundry Sand as well as the wear of two different grades of readily available steel bar stock. The test methodologies will be followed by the sieving and wet abrasive handling procedures.

4.2 Abrasive and Steel Samples

The Ottawa Foundry Sand used for all tests is as-shipped Barco 32 from Opta Minerals. The size distribution as-measured in the lab can be found in APPENDIX A on the information sheet supplied by the manufacturer. The steel round bar stock used as media samples were mild steel, AISI 1018, and high strength low alloy (HSLA) AISI 4140 heat-treated steel. The media samples cut from the round bar stock are 50 mm in diameter by 38 mm (2" x 1 ½"). They were cut using a cooled, abrasive chop saw, the Kalamazoo Industries K12-14W. The abrasive blades used, #116-12, were specifically hardness-rated for the steels used as media samples, medium stock.

4.3 SWAT Machine Settings

The SWAT Machine was run at three different applied force settings and four different rotational speeds. The force settings are controlled by the weight stack while the rotational speeds are set by the wall-mounted motor controller. They were 100, 250 and

500 N and 140, 155, 180, 195 RPM respectively. Upon completion of these sets of tests, they were repeated under wet conditions. This required only the addition of hoses to direct water into the test chamber. These hoses were used to keep the wheel of the SWAT Machine wet as the test progressed.

4.4 SWAT Machine Experimental Procedure

4.4.1 SWAT Machine Dry Procedure (SWAT Locked Cycle additional steps italicized)

Each test performed was subject to the exact same procedure. It was as follows:

1. Clean and weigh steel media sample
2. Load media sample into sample holder (in test chamber)
3. Load abrasive into ore bin
4. Set up abrasive collection bucket
5. Set up instrumentation for torque and strain measurement
6. Set desired applied force for test
7. Set appropriate wheel rotation speed
8. Start rotating wheel
9. Start dust collection system
10. Start data collection once wheel is up to speed
11. Open the ore bin's gate and allow the sand to flow into the test chamber
12. Ensure consistent sand curtain flows between wheel and media sample

13. Apply force to media sample and wheel by engaging the lever arm and lock in place

14. Record start time of test

15. Ensure sand flow remains constant, media sample remains restrained and data is being recorded

16. After experimental time expires, disengage the lever arm

17. Stop the sand flow and wheel rotation

18. Stop dust collector once air is free of fine particulate

19. Collect all sand remaining in test chamber, empty into collection bucket

20. Remove, clean and dry media sample

21. Record the mass of the media sample

22. Transfer torque and strain data to computer for appropriate processing

23. Calculate the mass loss from the two media sample mass readings

24. Calculate the average torque and strain experienced during the experiment

25. Identify the collected abrasive product and set aside for sieving

26. Screen product using standard procedure

27. Remove fine product (below 100 μm)

28. Replenish feed with equivalent mass of new abrasive

29. Repeat test

4.4.2 SWAT Machine Wet Procedure

The wet procedure mirrors that of the dry tests except for a few minor changes: there is no dust collection system required and the abrasive product must be dried before sieving. These changes are reflected in the updated steps mentioned below:

9. Start water system; ensure wheel is being washed appropriately

15. Ensure sand flow remains constant; no wet sand buildup blocks the flow, media sample remains restrained and data is being recorded

18. Stop water system, ensure wheel is clean and no particles remain

19. Wash out test chamber, collecting all sand remaining and empty into collection bucket

20. Start vacuum filter, to separate excess water from abrasive product

21. Remove, clean and dry media sample

22. Record the mass of media sample

23. Transfer torque and strain data to computer for appropriate processing

24. Calculate the mass loss from the two media sample mass readings

25. Calculate the average torque and strain experienced during the experiment

26. Identify the filtered, collected abrasive product and dry in oven for up to 24 hours

27. Set aside dried, collected abrasive product for sieving

4.4.3 SWAT Machine Slurry Procedure

The slurry procedure has been used only once, it was used when the abrasive product was too fine to effectively flow into the test chamber on its own (Hewitt, Allard et al.). A slurry of 40% solids was prepared before each test in order to keep the ore in suspension. This helped avoid any potential clogging or blocking of the ore delivery system, allowing for smooth operation and data collection. Below is the complete procedure:

1. Clean and weigh steel media sample
2. Load media sample into sample holder (in test chamber)
3. Set up abrasive collection bucket
4. Set up instrumentation for torque and strain measurement
5. Set desired applied force for test
6. Set appropriate wheel rotation speed
7. Mix process water and abrasive into slurry
8. Start rotating wheel
9. Start data collection once wheel is up to speed
10. Load slurry into ore bin and open gate to allow slurry to flow into test chamber
11. Apply force to media sample and wheel by engaging the lever arm and lock in place
12. Record start time of test
13. Ensure slurry flow remains constant, media sample remains restrained and data is being recorded

14. After experimental time expires, disengage the lever arm
15. Stop the wheel rotation
16. Allow slurry to completely drain from ore bin and clean all remaining residue
17. Wash out test chamber, collect all remaining slurry and empty into collection bucket
18. Start vacuum filter, to separate excess water from slurry
19. Remove, clean and dry media sample
20. Record the mass of the media sample
21. Transfer torque and strain data to computer for appropriate processing
22. Calculate the mass loss from the two media sample mass readings
23. Calculate the average torque and strain experienced during the experiment
24. Identify the filtered, collected abrasive product (slurry) and dry in oven for up to 24 hours
25. Set aside dried, collected abrasive product for sieving

4.5 Sieving Procedure

Sizing the abrasive product required two separate sieving steps, the first to size the coarse product, the second to size the finer product. There are two sets of sieves allowing for twice the material to be screened at once, the coarse sizing ranges from 600 to 300 μm, anything below that size is considered fine for this process, and is then screened down to 75 μm. The data collected from this sizing is used to determine Work Index (W_i) values for the various tests performed.

4.6 Wet Abrasive Product Handling

The wet abrasive product falls directly from the test chamber into a pail setup specifically for vacuum filtering; the bottom of the filter pail has been pierced to allow water to flow into a larger pail underneath. The larger pail has been retrofitted with a wet/dry vacuum attachment such that the laboratory's wet/dry vacuum can be attached and used as the vacuum source. The filter pail is lined with filter paper (6μm) to ensure no valuable product is lost. After filtering is completed, the sample and filter paper are placed on drying racks and loaded into an oven to dry. They dry at 74^{o}C (165^{o}F) for 18-24 hours, or until they are completely dry. Sizing of the newly dried product proceeds as mentioned above.

Chapter 5 RESULTS

5.1 Introduction

The first group of results will encompass data traditionally acquired from the SWAT Machine when used in the Total Media Wear Model. This will be followed by the data obtained through the new procedure and finally the data obtained by performing the Locked-cycle Test.

5.2 Total Media Wear Model Data

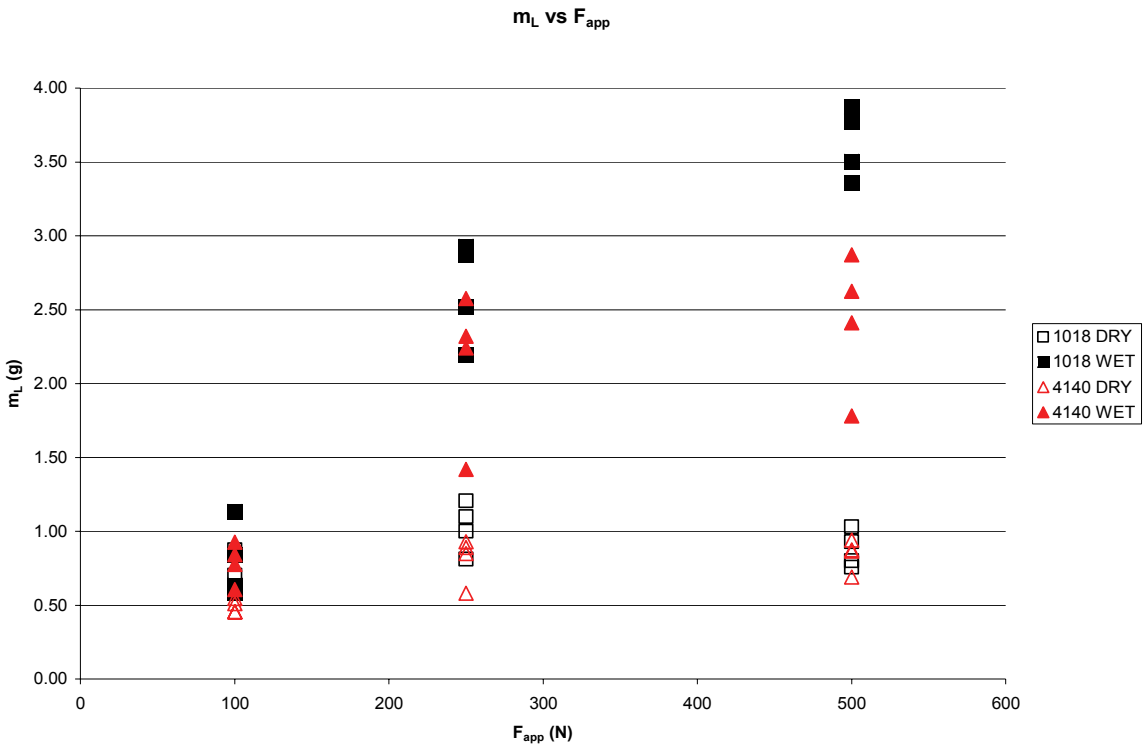

Figure 5.1: Steel media mass loss as a function of applied force.

Recall, the friction coefficient is calculated using equation (1), where T is the Torque in Nm, F_A is the applied force in N and r is the radius of the abrasion wheel in m. A higher μ value equates to a rougher surface and a higher frictional force would need to be

overcome in order to induce slipping. This is followed by the product size distribution; it is examined under the different operating conditions.

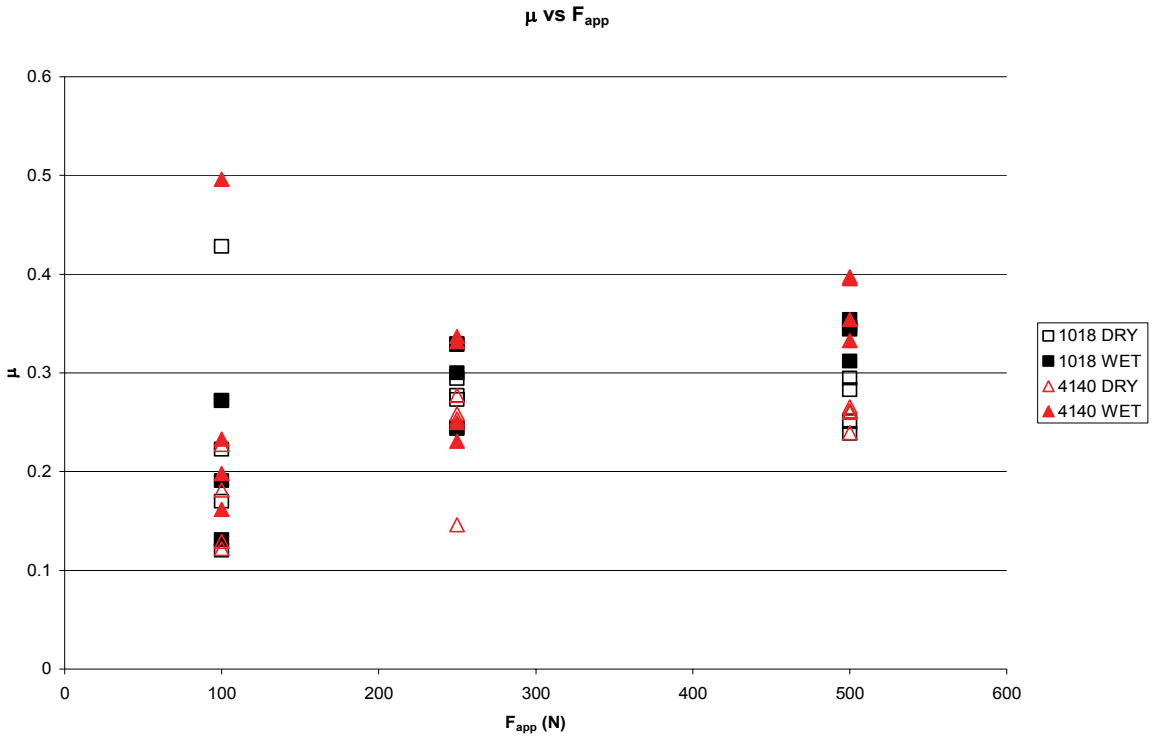

Figure 5.2: Coefficient of friction as a function of applied force.

5.3 SWAT Breakage Data

Figure 5.3 to Figure 5.12 represent the new Bond procedure using the SWAT Machine. This set of data creates size distribution charts for the feed and product and examines the relationships between the wear rate and rotational speed, as well as the applied force and specific energy calculated for the tests. Also, the W_i values have been calculated based on the energy added to the system, resulting in the exploration of relationships between W_i and the specific energy of the system.

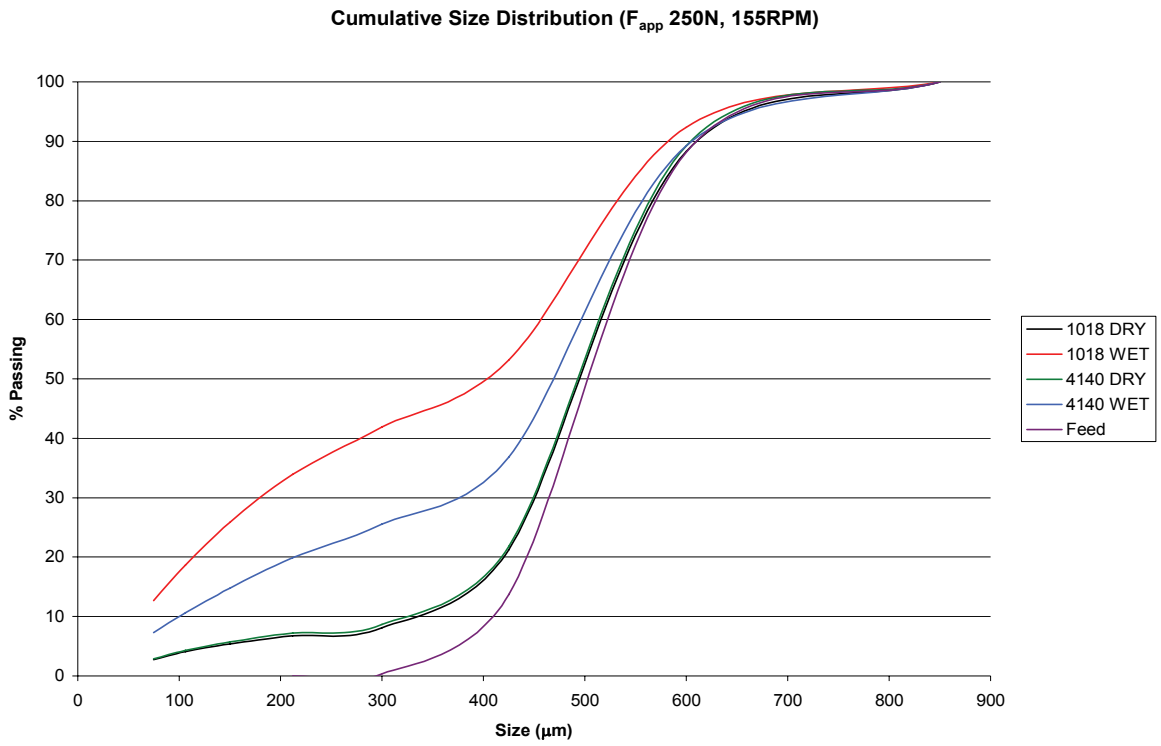

Figure 5.3: Product size distribution at 155 RPM and F_{app}: 250 N.

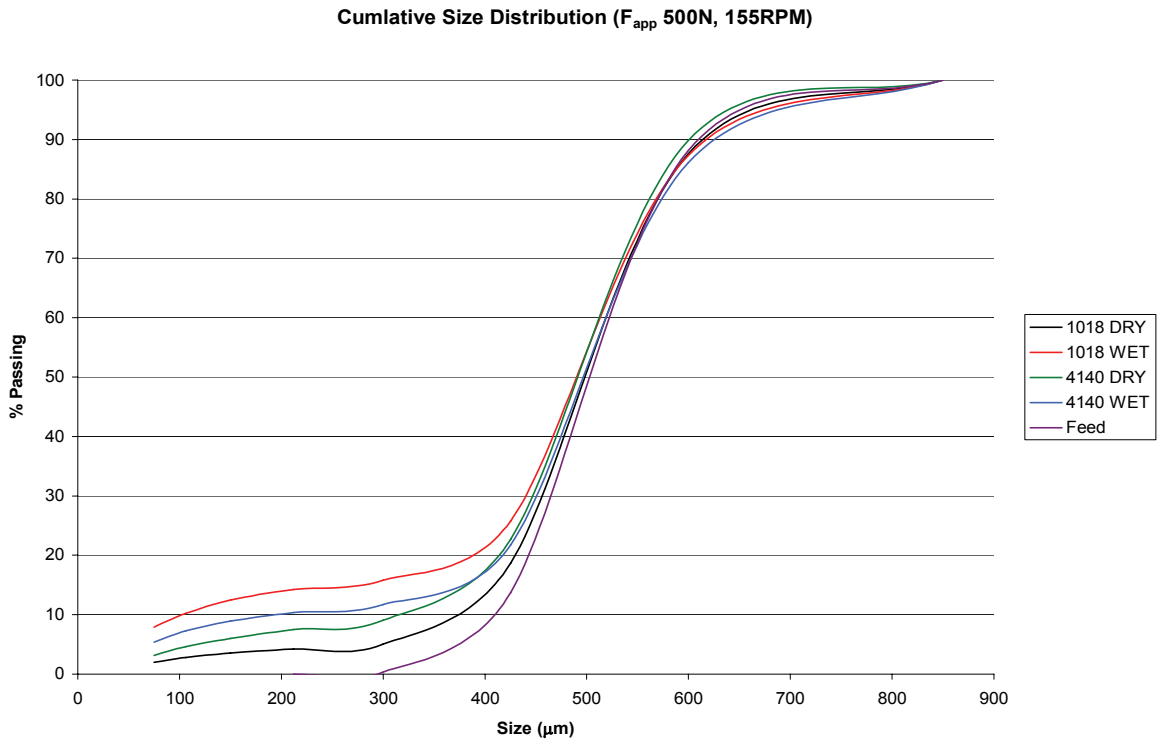

Figure 5.4: Product size distribution at 155 RPM and F_{app}: 500N.

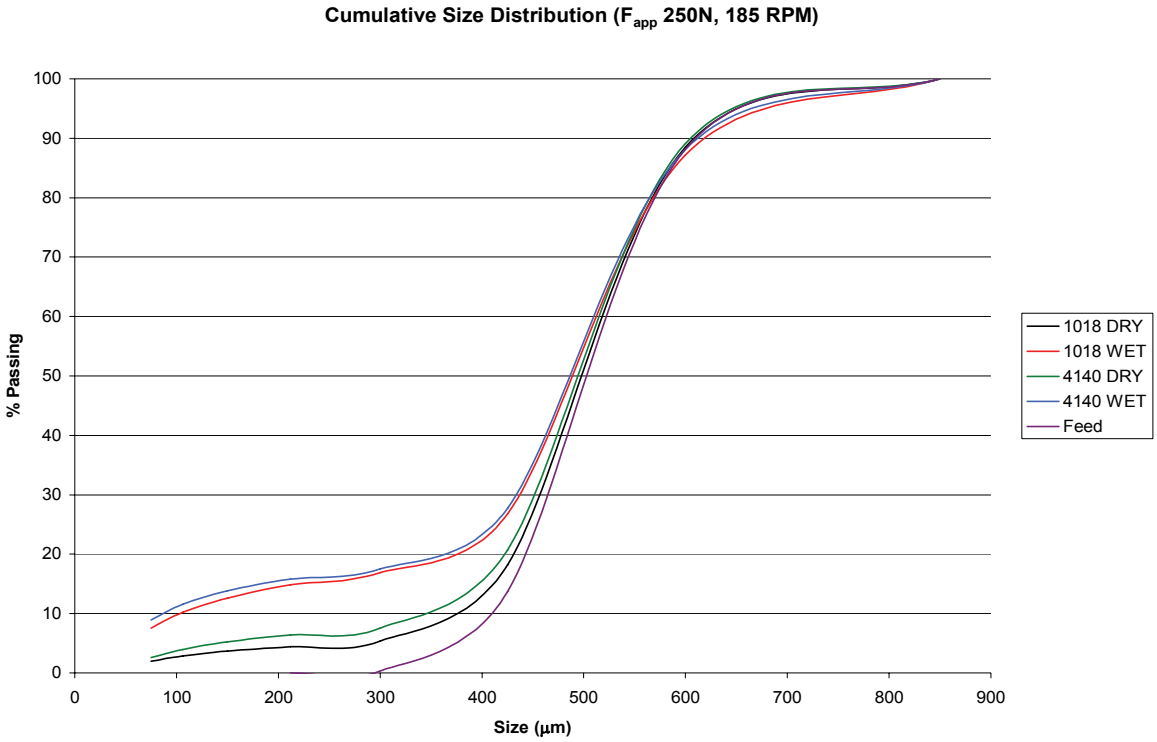

Figure 5.5: Product size distribution at 180 RPM and F_{app} 250N.

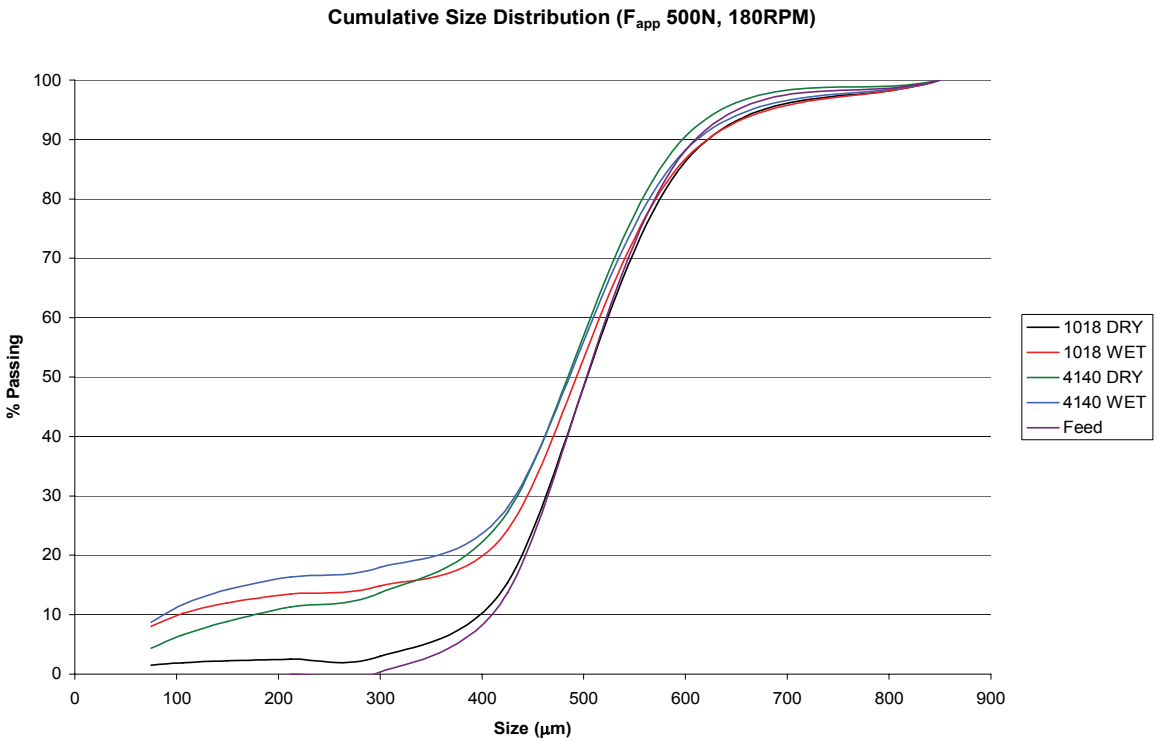

Figure 5.6: Product size distribution at 180 RPM and F_{app}: 500N.

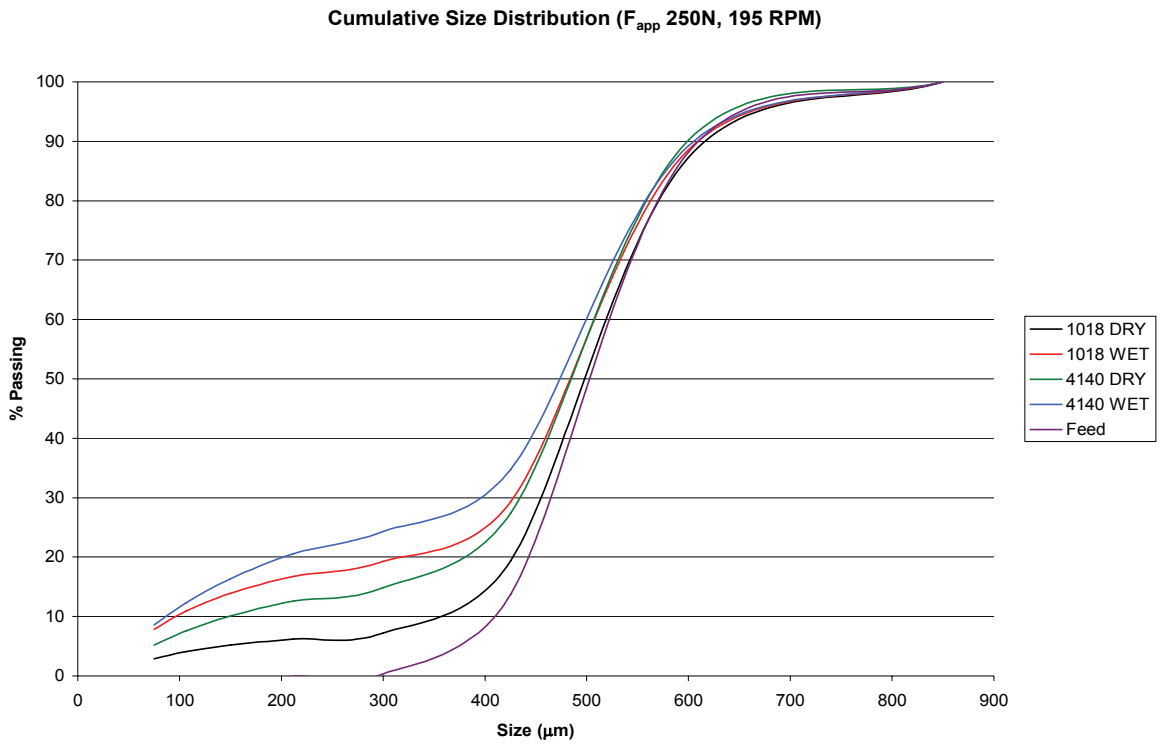

Figure 5.7: Product size distribution at 195 RPM and F_{app} 250N.

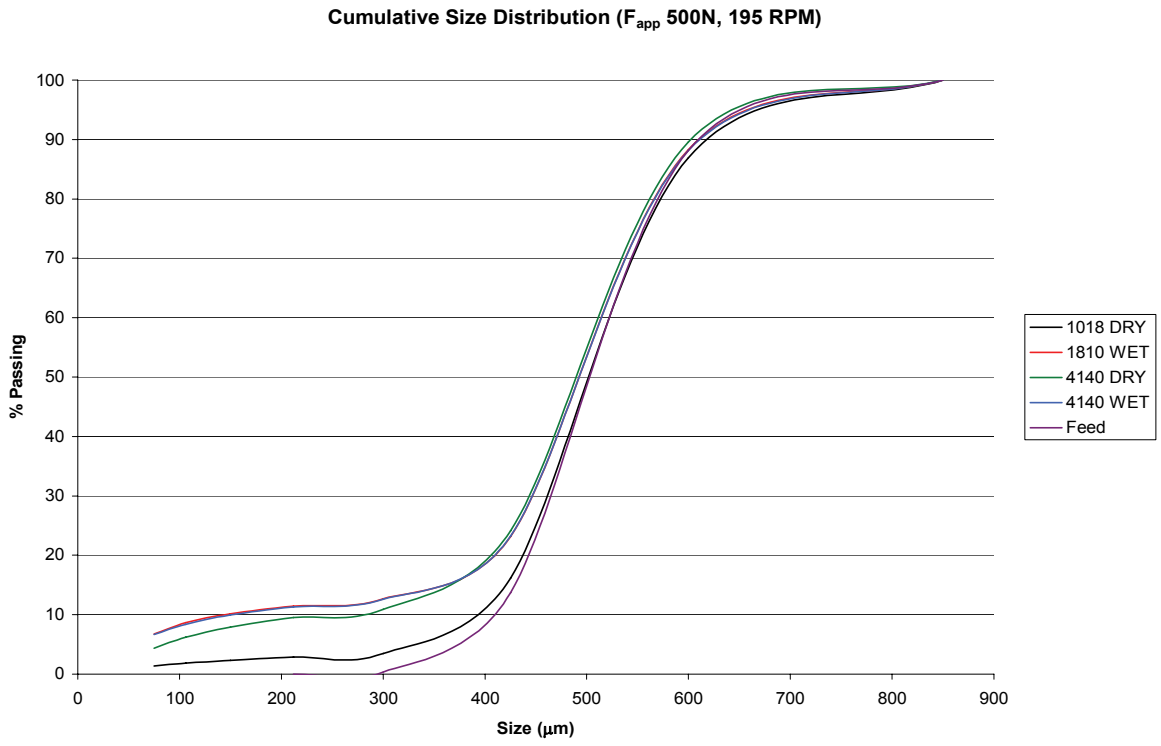

Figure 5.8: Product size distribution at 195 RPM and F_{app} 500N.

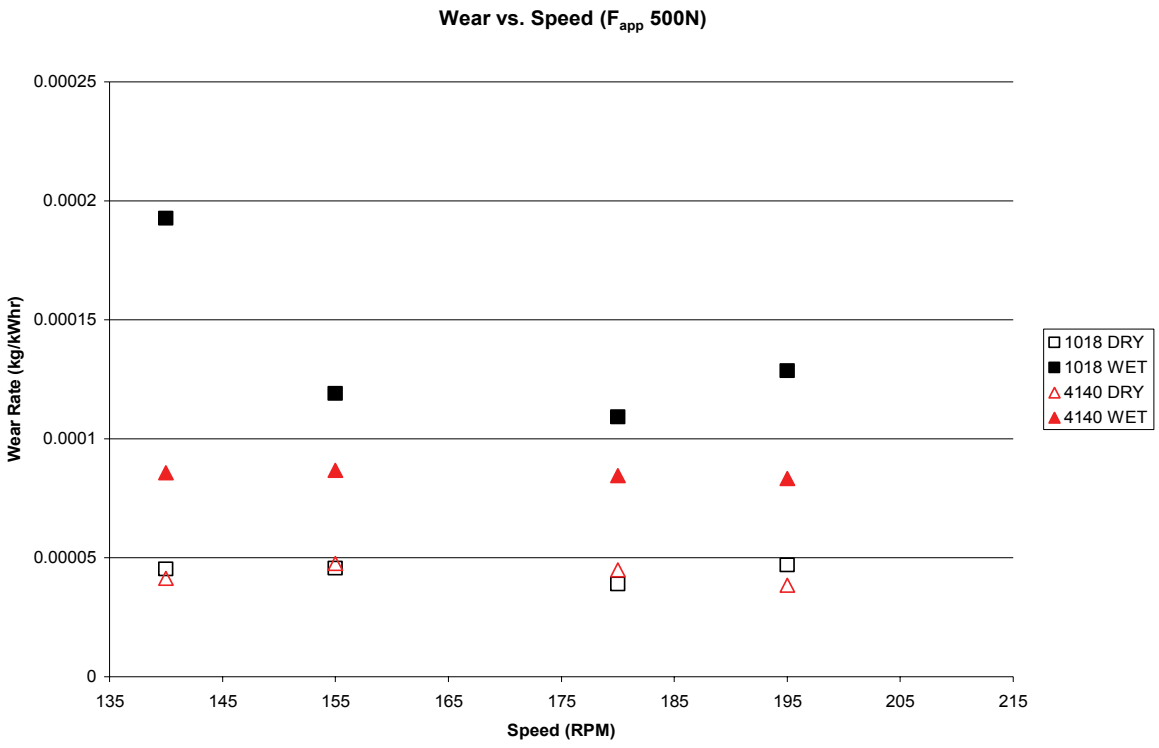

Figure 5.9: Steel media sample wear rate as a function of abrasion wheel rotational speed.

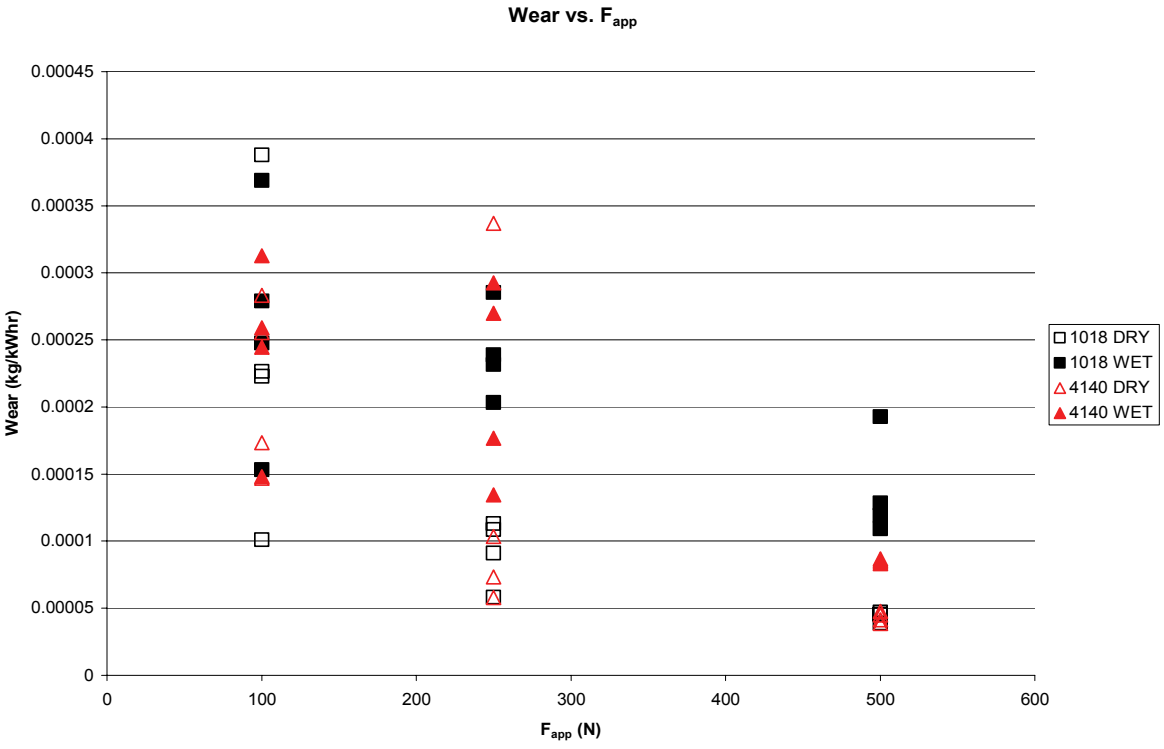

Figure 5.10: Steel media sample wear rate as a function of applied force.

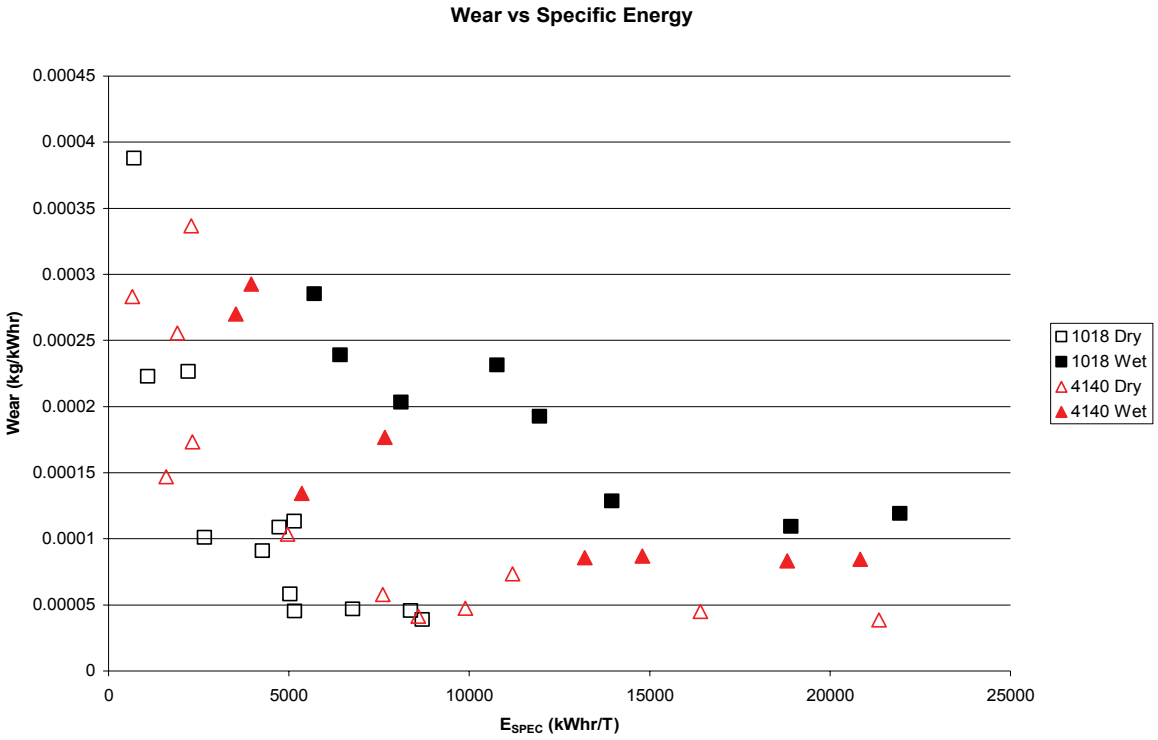

Figure 5.11: Steel media sample wear as a function of specific energy consumed.

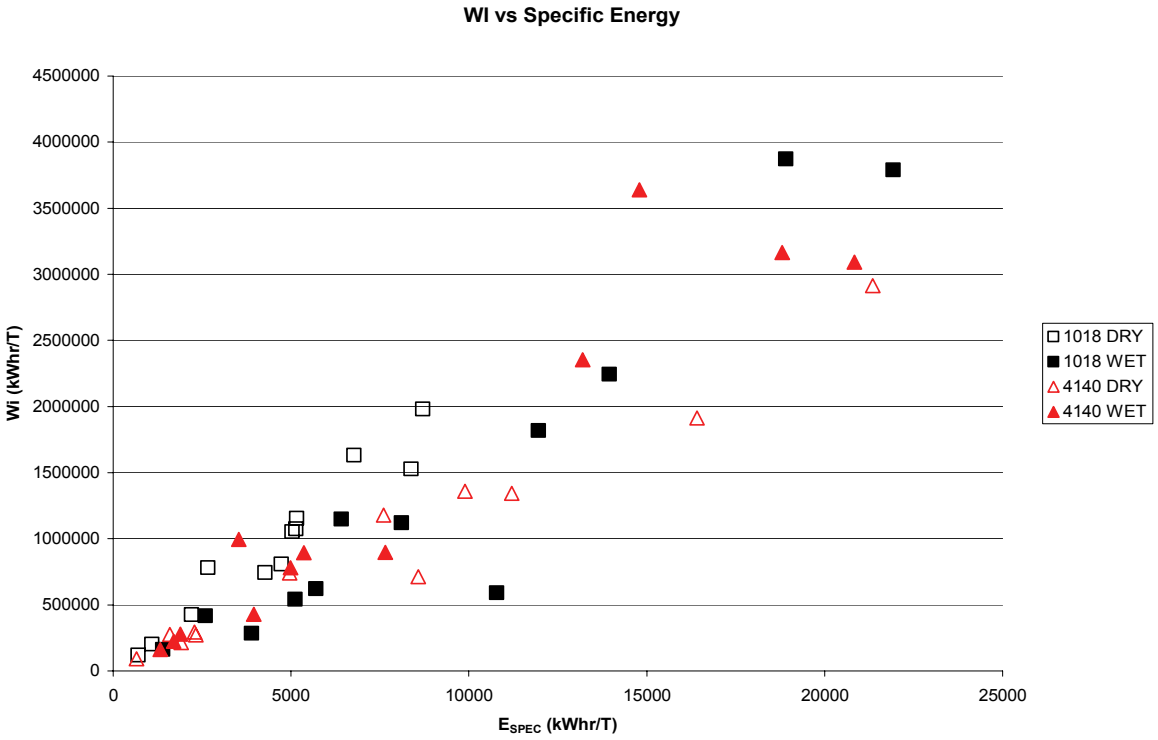

Figure 5.12: Abrasive W_i as a function of specific energy consumed.

5.4 SWAT Locked-cycle Test Data

Figure 5.13 to Figure 5.15 were generated from the results of a locked-cycle test. That is, the same abrasive product was used for eight consecutive tests, with fresh feed being added only to offset the fines screened out of the product. Data from the locked-cycle test is limited since it is performed at a single rotational speed and applied force. The focus of these particular results is how variables respond when subjected to testing with an abrasive whose size distribution is slowly evolving.

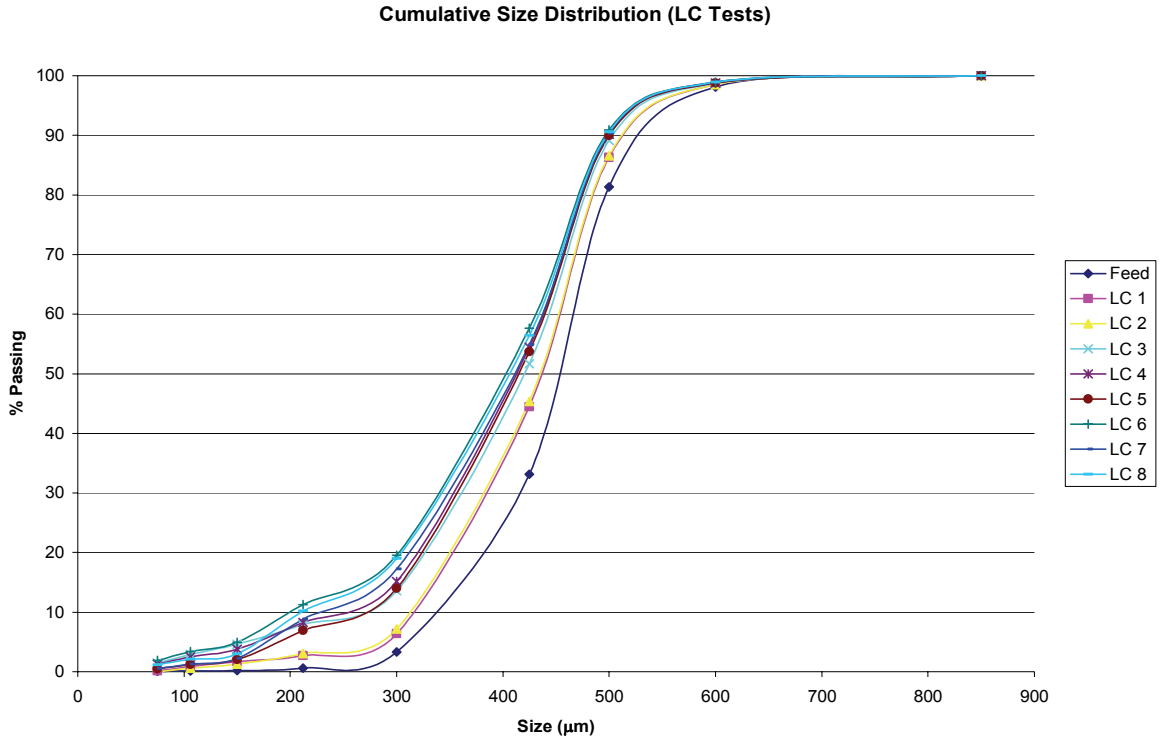

Figure 5.13: Locked-cycle test size distributions.

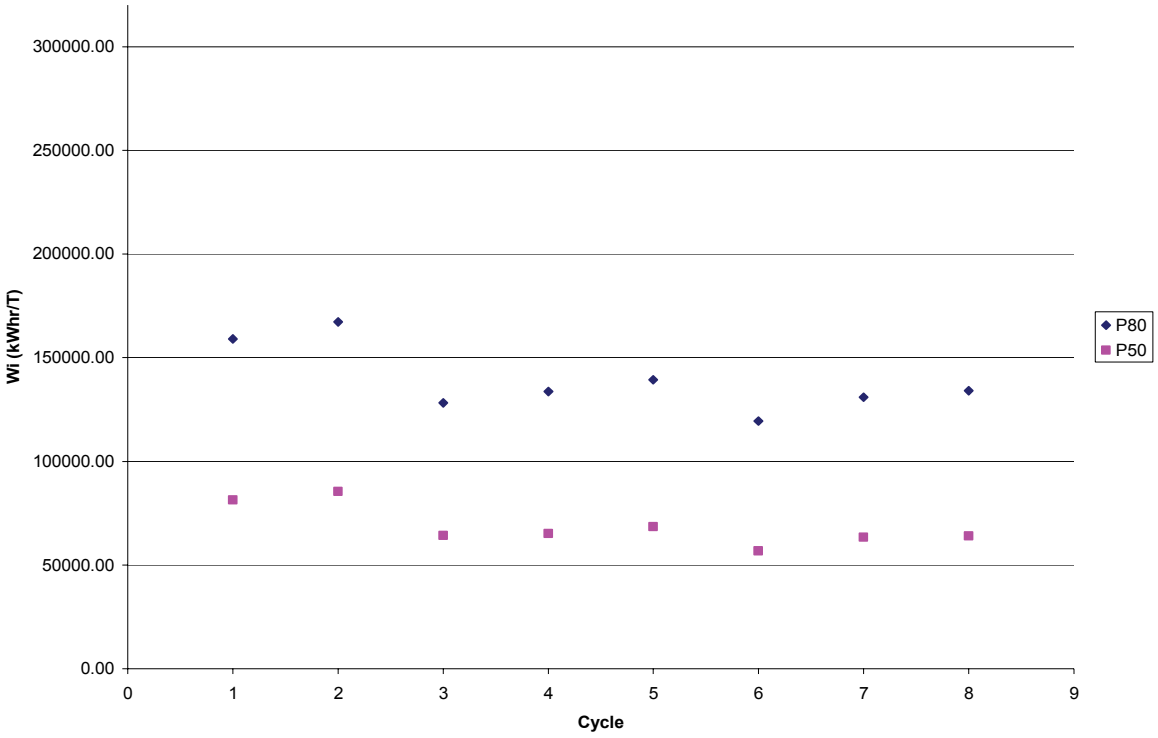

Figure 5.14: W_i evolution over locked-cycle tests.

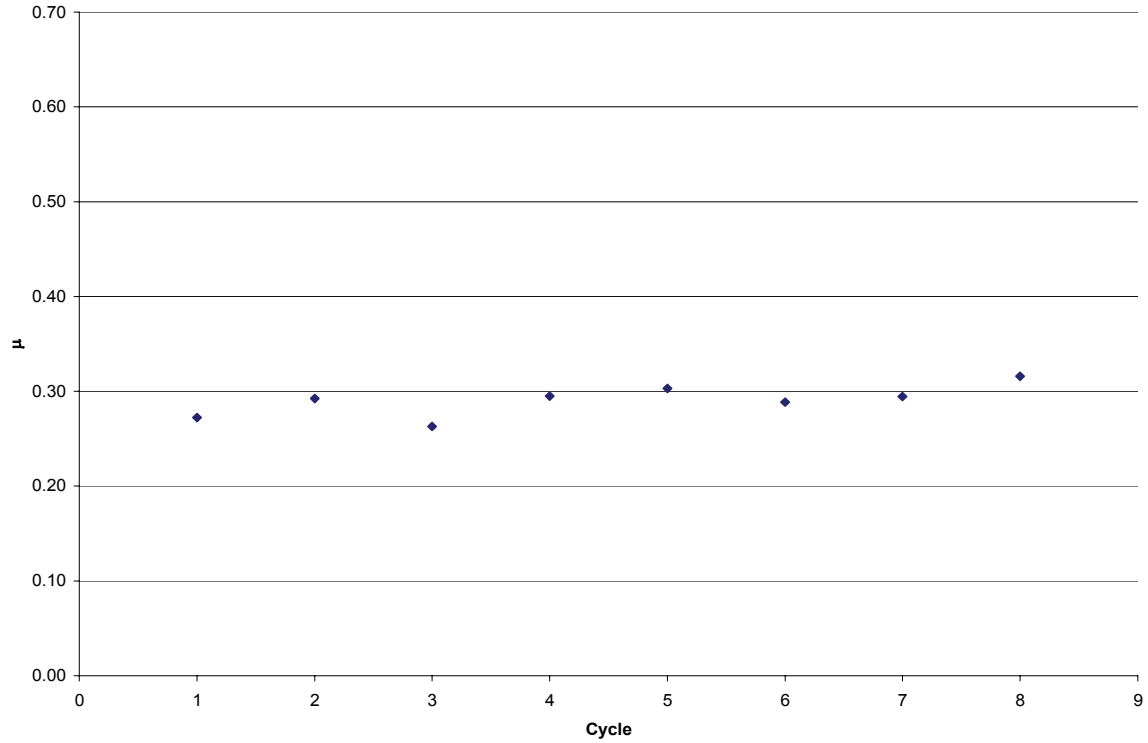

Figure 5.15: μ evolution over locked-cycle tests.

Chapter 6 DISCUSSION

6.1 Introduction

In the following section, the experimental results will be examined more closely in an attempt to better understand how the SWAT Machine can be used as an effective replacement for Bond Index testing in addition to its current use in the Total Media Wear Model.

6.2 Steel Media Samples and Abrasive Breakage

First, focusing on the mass loss of the steel media samples, it can be seen that there is a difference between wet and dry testing conditions. This has been observed and demonstrated graphically in past work. See Figure 6.1.

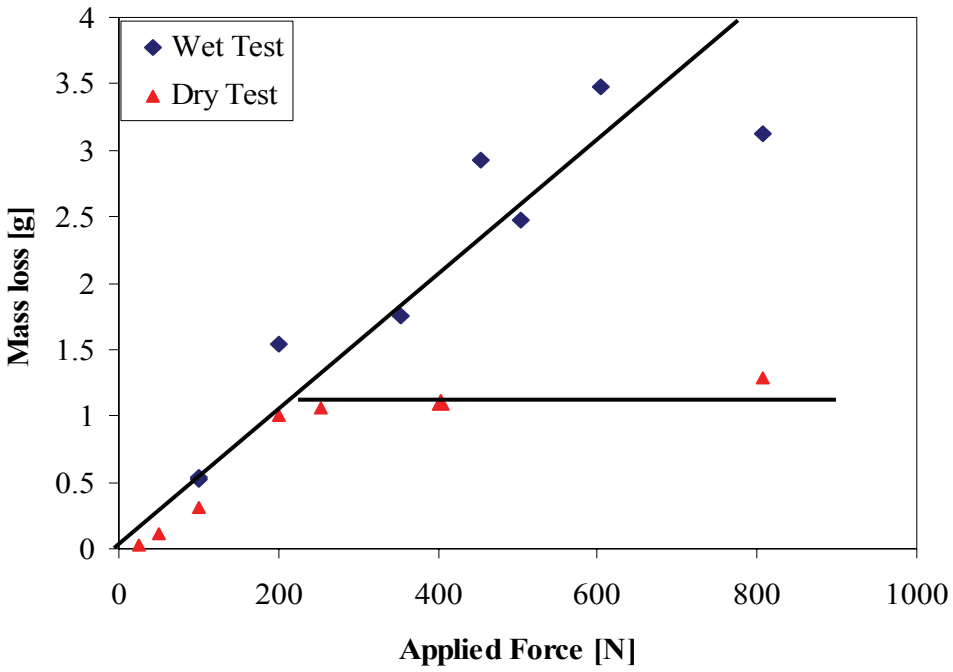

Figure 6.1: Wet abrasion test results for 1018 steel(Chenje 2007).

It can be seen that there is a point where the mass loss of the sample tends to level off when dry, but continues to increase when tested under wet conditions. This was also the case in the current results, in Figure 5.1. The wet tests for both steel types were subjected to higher mass loss than their dry test counterparts. Dry testing results in a slightly higher mass loss at the middle value, 250N. This was also evident in previous work discussed earlier (Radziszewski, Hewitt et al. 2008). The reasons for less wear under dry conditions at higher applied forces stem from the fact that under these higher loads scenarios, the pressure exerted onto the abrasive grains is extremely high, high enough to effectively grind or pulverize the material as it gets trapped between the two metallic surfaces. Lower applied forces do not readily grind the abrasive. In these cases there is the possibility for the abrasive grains to more effectively abrade the media samples. This can be achieved by the particles sliding or rolling across the surface, cutting into it. Aside from some minimal scatter, Figure 5.2 agrees with this statement. At lower force, there is a lower coefficient of friction, indicative that the abrasive particles are able to move more freely than at higher applied forces where they are trapped and ground between the steel surfaces. The evolution of abrasive size shown from Figure 5.3 to Figure 5.8 demonstrates the abrasive's response to different applied loads and wheel rotational speeds. The lowest curve on the graphs represents the abrasive feed size distribution, i.e., the abrasive before entering the SWAT Machine. Where this curve intersects the other curves effectively shows that the feed has successfully been broken into finer abrasive particles. This tends to happen at sizes above 500 μm. Another important observation is the fact that a greater percentage of fine abrasive particles are produced when performing the tests under wet conditions. It should be noted that this

curve represents the size sampling from each of the different bags used during the experiments. The final values of the size distribution do not exactly match the standard information supplied by the company in their information sheet, Appendix A.

6.3 System Energy and Wear Rate

Figure 5.9 demonstrates that the rotational speed of the abrasive wheel has little effect on the overall performance of the test. This confirms previous work performed in the lab (Radziszewski, Varadi et al. 2005). The dry tests for both types of steel media tested experienced similar wear rates regardless of the samples differences in physical properties (hardness) or rotational energy input to the system. The wet tests produced similar results. However, the wear rates were somewhat distanced even while considering the scatter present in the 1018 steel media sample. Overall, the important information to retain from Figure 5.9 is the relatively consistent wear rate present across different tests in which the input energies varied. The only other method to alter the energy of the system is by changing the applied force; this is demonstrated in Figure 5.10. The wear rates converge nicely as they approach the 500N upper limit of the tests. As mentioned earlier, when approaching this upper limit, energy put into the system is being channeled preferentially towards breaking the abrasive as opposed to abrading the steel media sample.

Figure 5.11 is without question cluttered; however, exponential decay curves demonstrate a reasonable fit. Figure 5.11 must first be broken down into separate graphs for each steel media type used, 1018 and 4140. Looking at Figure 6.2 and Figure 6.3; the steel

media samples, both wet and dry exhibit separate, but similar relationships. The dry tests tend to have a higher rate of decay than their wet counterparts. The statistical analysis of these observations follows below in Figure 6.4 through Figure 6.7. They were produced with the assistance of a software suite called Minitab 15. Each graph displays the line of best fit along with the 95% confidence interval, the standard deviation, correlation coefficient and the R-squared value.

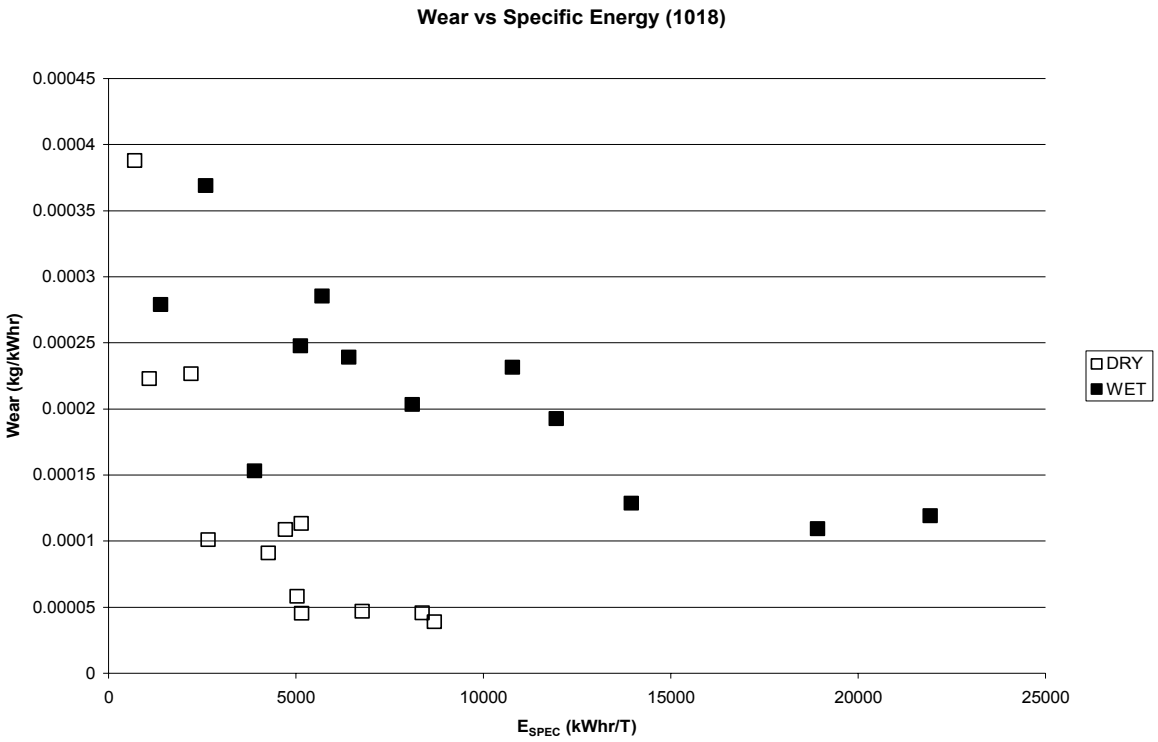

Figure 6.2: Steel media wear rate as a function of specific energy for 1018 steel.

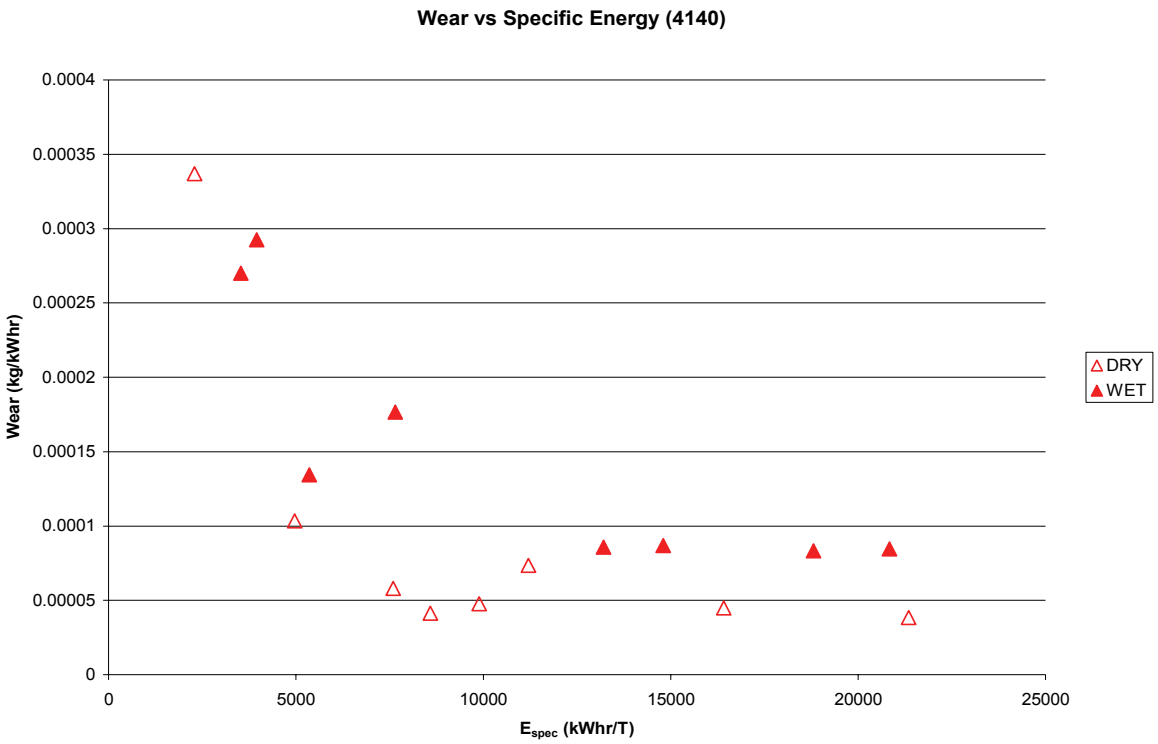

Figure 6.3: Steel media wear rate as a function of specific energy for 4140 steel.

It is evident that these regressions are by no means perfect or exact answers, but they do carry some weight. Further examination would be required to determine without a doubt the precise relationship these parameters play in the whole of the experiment. Correlations between 0.3 and 0.7 are said to exhibit some relationship, but the addition of other parameters may help in determining the actual relationship. It is unfortunate that there is visually a great deal of scatter in these figures; however, in some cases it tends to be well balanced, above and below the confidence limits. The steel media sample regressions for dry and wet tests are presented as separate models. Table 6-1 below displays the values obtained from the statistical analysis of dry and wet testing combined. Note that Minitab displays R-squared values as a percentage not a decimal.

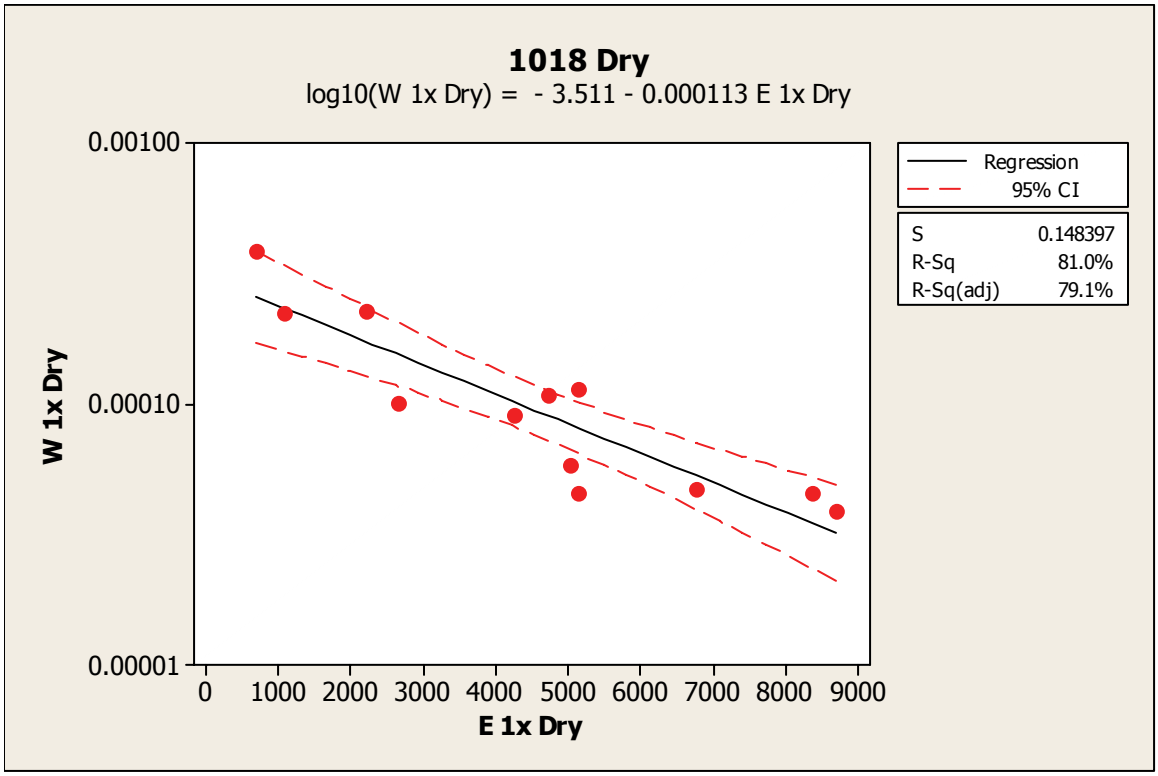

Figure 6.4: Line of best fit regression analysis for 1018 steel samples, dry only.

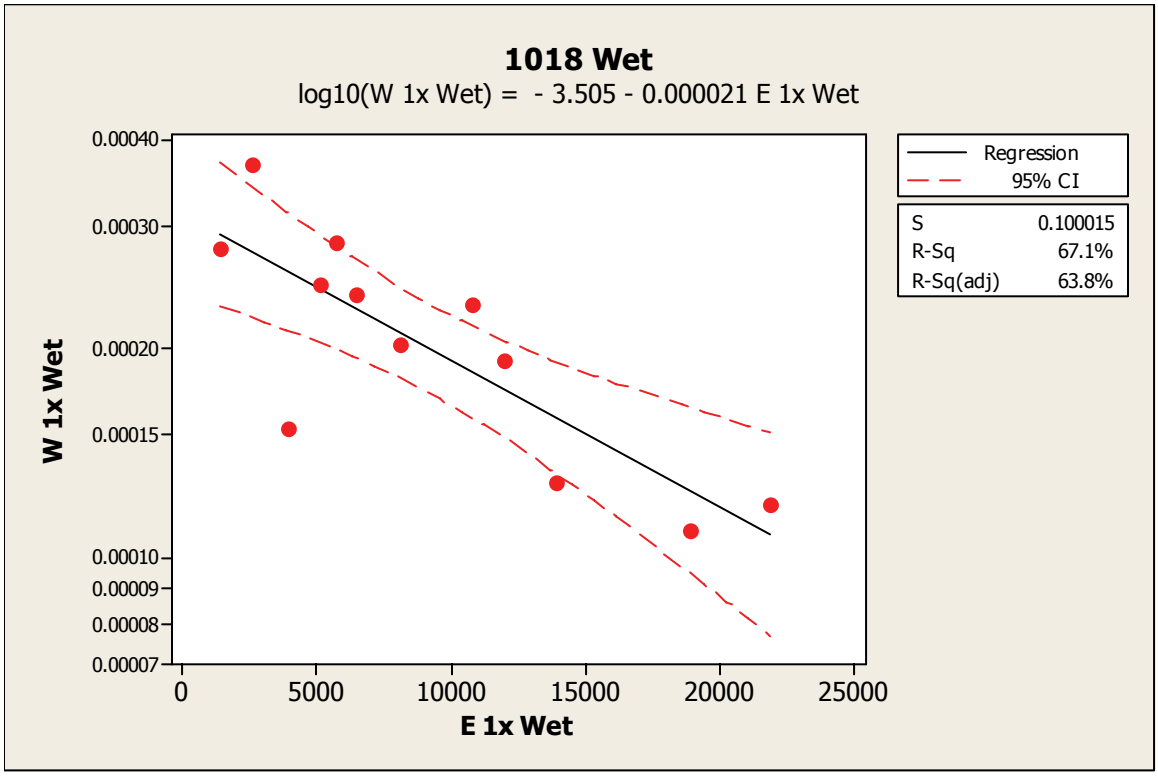

Figure 6.5: Line of best fit regression analysis for 1018 steel samples, wet only.

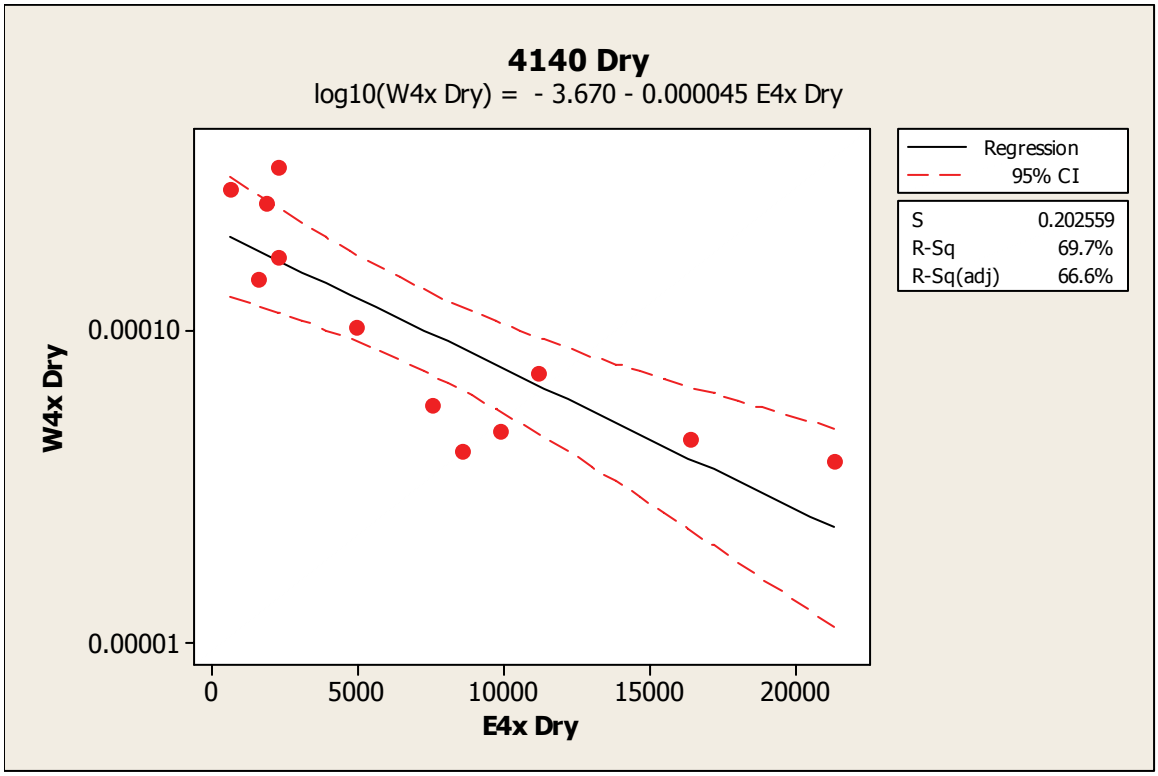

Figure 6.6: Line of best fit regression analysis for 4140 steel samples, dry only.

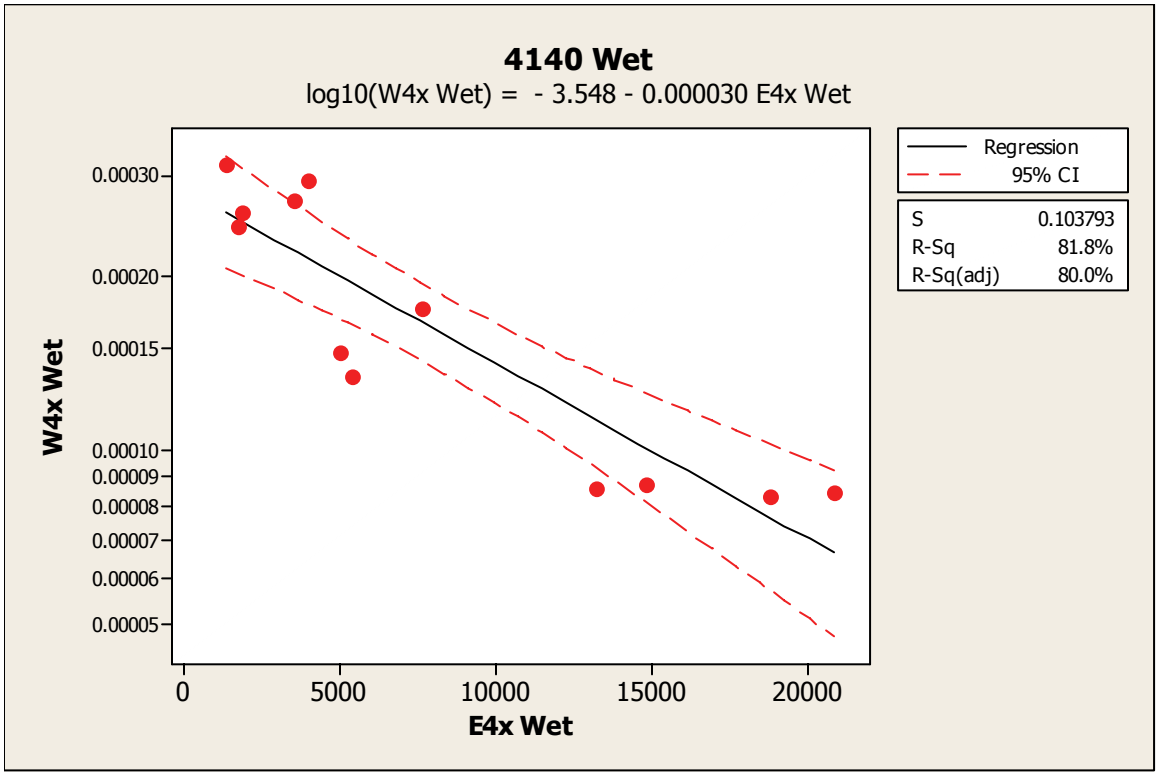

Figure 6.7: Line of best fit regression analysis for 4140 steel samples, wet only.

Table 6-1: Regression analysis performed for 1018 and 4140 steel media tests by Minitab 15.

	Steel Media	
	1018	**4140**
Slope	$\log_{10}(W1x) = -3.771 - 0.000013\ E\ 1x$	$\log_{10}(W4x) = -3.618 - 0.000036\ E\ 4x$
S	0.300355	0.202957
R^2	5.6	58.9
R^2_{adj}	1.3	57.0

Table 6-1 demonstrates that there is a greater fit achieved by exploring relationships with four separate statistical tests. Wet and dry testing for 1018 steel samples are without a doubt, separate and distinct models. The 4140 tests can be viewed as similar; however, the statement cannot be made with the same level of confidence.

6.4 Work Index

Finally, in Figure 5.12, the values for the Work Index have been calculated and are presented against the specific energy calculated for each individual test. Four distinct linear functions can be seen, one for each type of steel media used and for each test condition, dry and wet. Figure 6.8 revisits Figure 5.12, but with the addition of regression lines. The analysis of all four lines follows in Table 6-2.

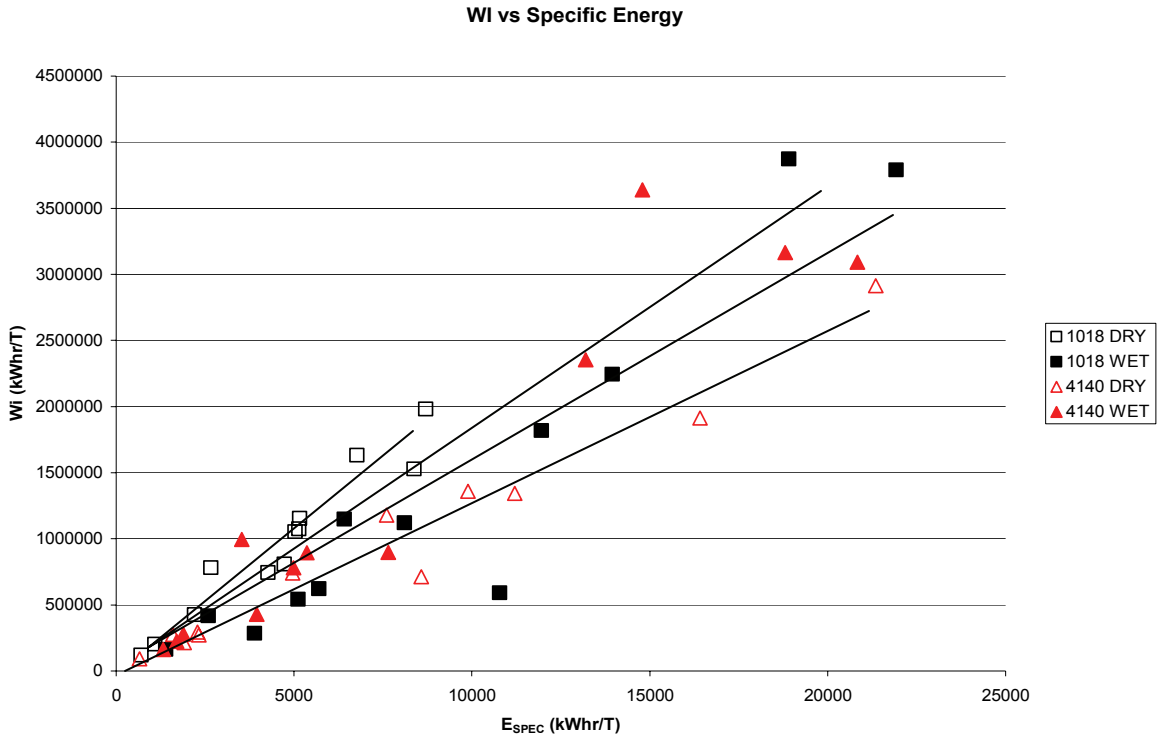

Figure 6.8: Linear relationship demonstrated for work index as a function of specific energy.

Table 6-2: Regression analysis for Figure 5.12 (Figure 6.8).

	1018		4140	
	DRY	WET	DRY	WET
Slope	$W_i = 211.475\ E_{spec}$	$W_i = 184.786\ E_{spec}$	$W_i = 127.722\ E_{spec}$	$W_i = 174.925\ E_{spec}$
R	0.973	0.950	0.983	0.952
R^2	0.946	0.903	0.967	0.907

The correlation coefficient and R-squared values are very high for these four lines, indicating a strong relationship between the specific energy calculated in the system and the calculated Work Index value. The 4140 wet test slope is steeper than the dry test suggesting that less energy would be required during wet testing to achieve the same Work Index value. This theory is consistent with existing literature (Tuzun 2001); however, in laboratory mill tests, dry grinding requires 1.3 times the energy as wet

grinding. Examining the two slopes, dry grinding would require 1.37 times the energy (E_{spec}) to achieve the same W_i value under these conditions. Unfortunately, the 1018 tests do not agree under the same circumstances. By looking at the data in Table 6-2, the dry grinding appears to require less energy than the wet tests. With the relatively new implementation of wet testing in the laboratory, there may be issues with variability and process control that must be addressed in the future; these will be discussed in further detail in the recommendations and conclusions, shortly.

6.5 Global Dry/Wet Test Observations

Examining these results further has produced the following useful information:

During dry tests, there is a transition zone dependant on the applied force experienced by the media sample. Below 250N, it is evident that the wear rate (per unit energy) increases, resulting in greater sample wear. This is caused by the abrasive being able to roll and abrade the steel surfaces. Increasing the applied force above this threshold value result in less wear and greater abrasive breakage, this is well documented in the results seen as lower or constant sample mass loss (Figure 5.1) at higher forces, the relatively constant coefficient of friction (Figure 5.2), the decrease in wear rate with respect to applied force and specific energy consumed by the system (Figure 5.10 and Figure 5.11 respectively).

Interestingly enough, there is no threshold value for wet tests; the mass loss will increase readily as the applied force increases. But all other trends previously stated will remain

intact. As the applied force increases, values, both measured and calculated, tend to converge resulting in less scatter and better results.

6.6 Locked Cycle Test

Figure 5.13 shows the size distribution evolution over the eight tests, ideally, the last cycle would have the size distribution with the greatest proportion of fines; however, cycles 6 and 8 are both very close and compete for that distinction. It is obvious that there is a change in product size. The increase of finer material is evident from the very first test. These results agree with the preliminary results displayed in Figure 3.4. The particles sized 425 μm represent roughly 1/3 of the feed, whereas after the first test they represent almost 45% and over 55% by the eighth test. This falls within a range of particle size that, visibly, is most readily broken, 350-450 μm.

Focusing on the Work Index now, recall Figure 3.5, acknowledging the presence scatter, a trend was alluded to that was a slight decrease in W_i as more cycles were completed. This is consistent with the newly acquired data seen in Figure 5.14. One very interesting note, the W_i values decrease over the eight cycles, numerically, there is roughly a 20% decrease in Wi from the first cycle to the last for both the P_{80} and P_{50} values. While preparing the results, however, it was noticed that W_i values increase in discrete blocks (cycles 1-2, 3-5, 6-8). There is no understanding or justification for this behaviour at this time. Perhaps further exploration of the Locked-cycle test will reveal more information about this occurrence.

Finally, Figure 5.15 displays the results for the friction coefficient calculated for each of the cycle tests. This data is not in agreement with the initial data set. Figure 3.6 shows a decrease in the friction coefficient during the four cycles performed in that data set. Current data suggests the opposite, that the coefficient will increase slightly over the course of the cycle tests. Across the four cycles in the preliminary test, the friction coefficient decreases by almost one third of its value. The new data increases by one tenth of its value over the first four cycles showing a more moderate increase overall. As noted with the data presented in Figure 5.14, the data can be examined in discreet sets because it has a slight periodic tendency. As discussed earlier, a decrease in friction coefficient was expected given the fact that the size distribution of the feed becomes finer over the course of the Locked-cycle test. Further study is required in order to determine the relevance of these observations.

6.7 Standard Deviation

The Relative Standard Deviation has been calculated for the data collected and calculated. It is displayed in tables according steel media sample type and test method. A brief discussion follows the tables displaying the sample mass loss, friction coefficient, wear rate, Bond Work Index and energy. Values are reported randomly for the test work performed. Boxes with numbers have two separate numbers where the top number represents the number of tests performed for that particular set of variables, and the number below is the relative standard deviation for the set of variables.

Table 6-3: Relative standard deviation of sample mass loss values for 1018 dry and wet tests respectively.

		Applied Force (N)		
	# Tests RSD	100	250	500
Speed (RPM)	140		5 39.63%	
	155	6 24.73%		
	180			5 25.60%
	195		2 2.07%	

		Applied Force (N)		
	# Tests RSD	100	250	500
Speed (RPM)	140		2 1.59%	
	155	2 5.17%		
	180			2 4.14%
	195		2 3.75%	

Table 6-4: Relative standard deviation of sample mass loss values for 4140 dry and wet tests respectively.

		Applied Force (N)		
	# Tests RSD	100	250	500
Speed (RPM)	140			5 13.15%
	155		5 8.60%	
	180	2 13.73%		
	195			2 2.86%

		Applied Force (N)		
	# Tests RSD	100	250	500
Speed (RPM)	140			5 6.18%
	155		5 6.25%	
	180	2 13.55%		
	195			2 16.38%

Table 6-5: Relative standard deviation of friction coefficient values for 1018 dry and wet tests respectively.

		Applied Force (N)		
	# Tests RSD	100	250	500
Speed (RPM)	140		5 8.73%	
	155	6 18.16%		
	180			5 4.82%
	195		2 1.95%	

		Applied Force (N)		
	# Tests RSD	100	250	500
Speed (RPM)	140		2 1.08%	
	155	2 4.40%		
	180			2 8.30%
	195		2 4.28%	

Table 6-6: Relative standard deviation of friction coefficient values for 4140 dry and wet tests respectively.

		Applied Force (N)		
	# Tests RSD	100	250	500
Speed (RPM)	140			5 3.23%
	155		5 0.54%	
	180	2 9.18%		
	195			2 0.55%

		Applied Force (N)		
	# Tests RSD	100	250	500
Speed (RPM)	140			5 12.31%
	155		5 31.74%	
	180	2 18.88%		
	195			2 2.61%

Table 6-7: Relative standard deviation of wear rate values for 1018 dry and wet tests respectively.

		Applied Force (N)		
	# Tests RSD	100	250	500
Speed (RPM)	140		5 46.55%	
	155	6 43.64%		
	180			5 21.73%
	195		2 4.02%	

		Applied Force (N)		
	# Tests RSD	100	250	500
Speed (RPM)	140		2 0.52%	
	155	2 0.77%		
	180			2 12.82%
	195		2 0.52%	

Table 6-8: Relative standard deviation of wear rate values for 4140 dry and wet tests respectively.

		Applied Force (N)		
	# Tests RSD	100	250	500
Speed (RPM)	140			5 12.02%
	155		5 9.14%	
	180	2 4.60%		
	195			2 3.41%

		Applied Force (N)		
	# Tests RSD	100	250	500
Speed (RPM)	140			5 6.18%
	155		5 37.26%	
	180	2 5.47%		
	195			2 18.90%

Table 6-9: Relative standard deviation of work index values for 1018 dry and wet tests respectively.

	Applied Force (N)			
Speed (RPM)	# Tests RSD	100	250	500
	140		5 35.43%	
	155	6 31.71%		
	180			5 23.70%
	195		2 15.35%	

	Applied Force (N)			
Speed (RPM)	# Tests RSD	100	250	500
	140		2 15.80%	
	155	2 8.18%		
	180			2 5.73%
	195		2 1.62%	

Table 6-10: Relative standard deviation of work index values for 4140 dry and wet tests respectively.

	Applied Force (N)			
Speed (RPM)	# Tests RSD	100	250	500
	140	2	2	5 11.06%
	155	2	5 4.99%	2
	180	2 8.06%	2	2
	195	2	2	2 3.12%

	Applied Force (N)			
Speed (RPM)	# Tests RSD	100	250	500
	140	2	2	5 1.12%
	155	2	5 20.07%	2
	180	2 35.58%	2	2
	195	2	2	2 7.91%

It is evident that some values displayed are alarmingly high. Certain aspects of this test procedure remain difficult to control, mainly the flow rate of abrasive and water remain the most complex and difficult to maintain perfectly constant. Many of the calculated values rely on the data being normalized for the amount of abrasive. The following data tables demonstrate this. Table 6-11 and Table 6-12 show the relative standard deviation values for the energy input into the system (kWhr). This is a simple calculation requiring the torque felt at the drive shaft, the applied force on the sample, the rotational speed of the wheel, etc. These values tend to fall within the acceptable range (up to 10% relatives

standard deviation). Now, turning to Table 6-13 and Table 6-14, the standard deviation values are much higher in most cases. They are the specific energy values calculated for each test. They represent the amount of energy added to the system as mentioned before, but now normalized for the amount of abrasive that passed through the test chamber (kWhr/T). With the abrasive allowed to flow freely and in generous proportions to ensure constant abrasive wear and breakage between the steel media sample and the wheel, it remains a challenge to run tests with consistent abrasive mass values. And since many of the calculated values rely on this measured abrasive mass value, the deviation from variable to variable is very sensitive to these changes.

Table 6-11: Relative standard deviation of energy input values for 1018 dry and wet tests respectively.

		Applied Force (N)		
	# Tests RSD	100	250	500
Speed (RPM)	140	2	5 8.73%	2
	155	6 18.16%	2	2
	180	2	2	5 4.82%
	195	2	2 1.95%	2

		Applied Force (N)		
	# Tests RSD	100	250	500
Speed (RPM)	140	2	2 1.08%	2
	155	2 4.40%	2	2
	180	2	2	2 8.30%
	195	2	2 4.28%	2

Table 6-12: Relative standard deviation of energy input values for 4140 dry and wet tests respectively.

		Applied Force (N)		
	# Tests RSD	100	250	500
Speed (RPM)	140	2	2	5 3.23
	155	2	5 0.54%	2
	180	2 9.18%	2	2
	195	2	2	2 0.55%

		Applied Force (N)		
	# Tests RSD	100	250	500
Speed (RPM)	140	2	2	5 12.31%
	155	2	5 31.74%	2
	180	2 18.88%	2	2
	195	2	2	2 2.61%

Table 6-13: Relative standard deviation of specific energy input values for 1018 dry and wet tests respectively.

		Applied Force (N)		
Speed (RPM)	# Tests RSD	100	250	500
	140	2	5 34.99%	2
	155	6 19.13%	2	2
	180	2	2	5 21.61%
	195	2	2 11.13%	2

		Applied Force (N)		
Speed (RPM)	# Tests RSD	100	250	500
	140	2	2 42.45%	2
	155	2 49.77%	2	2
	180	2	2	2 0.96%
	195	2	2 16.16%	2

Table 6-14: Relative standard deviation of specific energy input values for 4140 dry and wet tests respectively.

		Applied Force (N)		
Speed (RPM)	# Tests RSD	100	250	500
	140	2	2	5 8.30%
	155	2	5 2.76%	2
	180	2 16.91%	2	2
	195	2	2	2 0.47%

		Applied Force (N)		
Speed (RPM)	# Tests RSD	100	250	500
	140	2	2	5 23.19%
	155	2	5 20.11%	2
	180	2 33.75%	2	2
	195	2	2	2 11.99%

Chapter 7 CONCLUSIONS AND RECOMMENDATIONS

7.1 Introduction

In this final section, the goals of this work will be revisited in an effort to answer all questions related to this body of work. Recommendations for future work and newly outlined procedures will follow the closing remarks pertaining to this experimental work.

7.2 Conclusions

The goals of this experimental work were to explore the possibility of combining two pre-existing test procedures in order to create a single test that would generate steel media wear and ore breakage information for mill operators. This was achieved by:

1. Understanding abrasive wear and how it is predicted
2. Investigating how ore breakage can be studied with similar test methodologies
3. Examining and understanding abrasive wear and breakage under varied conditions using the SWAT Machine
4. Proposing a methodology for testing abrasive wear and ore breakage using the SWAT Machine

The following conclusions have been compiled in light of meeting these four objectives:

7.2.1 Ore Breakage

Breakage had been assumed to occur to any particle that was forced between the steel media and the steel wheel. Results tend to agree with this statement at high applied forces; however, questions remain concerning lower applied forces. This is illustrated in

Figure 5.1 and Figure 5.10 where higher sample mass loss and wear rates were found at lower applied forces than at higher applied forces. There is a transition near the applied force of 250N where sample mass loss levels off, wear rates decrease and breakage increases. Breakage occurs most efficiently above the transition energy; the energy transfer being more efficient. Below the transition, the energy transfer is not as efficient, with some going to breakage and some going to abrasive wear.

7.2.2 Test Methodology

The dry test methodology requires no important changes from the current setup; however, better abrasive delivery and dust control are possible, but not necessary. As for the wet test, better feed and water delivery control and wet filtering are needed. The SWAT Machine setup previously used had a number of issues that were addressed for this work. Further improvements must be made in controlling abrasive and water flow, as well as creating a more permanent solution for product filtering. A pressure filter system would perform much efficiently than the vacuum filter currently used.

7.2.3 Energy Requirements

While the Bond Work Index terms calculated for these tests are orders of magnitude higher than the typical Bond values, there exists a strong linear relationship between the specific energy of the system and W_i. As the SWAT breakage database grows, it will become a simple calculation to determine the W_i value for new materials. This will

effectively streamline the lab work required to determine the Work Index all while generating wear data for the operation at the same time. Overall, considering a traditional Bond Test will take 16 hours to complete properly, and having completed SWAT Locked-cycle tests in under 9 hours, this will reduce the time taken to obtain these values by around 50%. Finally, as modifications are made to the database and test apparatus, it should be able to be used as an in-line test procedure allowing for mill productivity to be maintained.

7.3 Recommendations for Future Work

While dry testing has been demonstrated to be repeatable and the data collected reliable (Chenje 2007), this is the first time any large scale testing was performed using the wet procedure. And as expected, there were some adjustments that had to be made before full scale testing was implemented. Recall Figure 2.2, the design of the SWAT Machine allowed for the use of water to flow into the test chamber and dampen the wheel before it came into contact with the steel media sample and the abrasive. Not until full scale testing was it noticed that the water could easily clog the abrasive nozzle. This happened through the capillary action as water is attracted to the space between the dry abrasive particles. The result is a complete halt in the flow of the abrasive, effectively ruining the test data. Any reduction in the abrasive flow rate potentially causes the steel wheel and media sample to come into contact with one another promoting steel on steel wear, undesirable to the outcome of the testing.

Another problem noted was that the brush used to clean the wheel of any remaining particles was trapping the fine abrasive particles, as seen in Figure 7.1. This had the potential to skew the results in terms of the size distribution of the product and the Work Index term calculated.

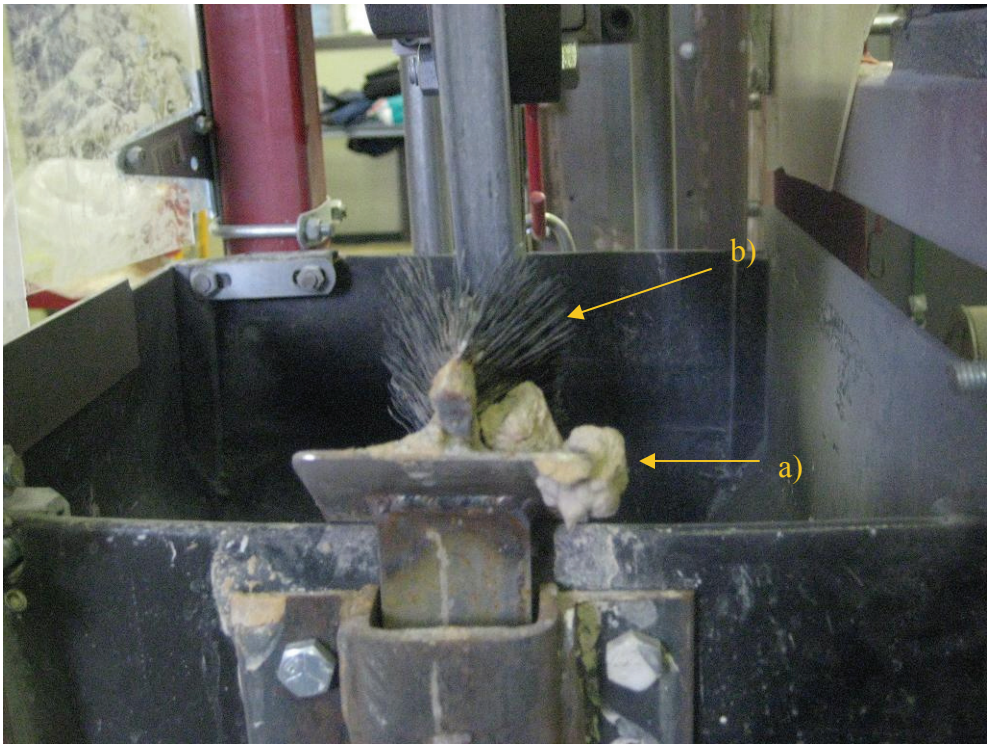

Figure 7.1: Fines, a), trapped in wheel brush, b), from traditional wet testing.

The solution to these two problems was found by altering the way in which water was delivered to the system. Instead of a trickle of water wetting the top of the wheel near the abrasive feed, modifications were brought to the area below the wheel. Water is now sprayed liberally onto the bottom of the wheel. This both wets the wheel and washes off any remaining abrasive particles that could have potentially been exposed to the applied forces and steel media sample repeatedly. The brush was also replaced with a large rubber flap on which the fines could land on, and then fall back into the hopper. Figure

7.2 below shows the new wet test setup, consisting of nozzles to flush abrasive particles and keep the wheel wet and the rubber flap (bottom left) keeping all of the fines contained within the test chamber. While this resembles a permanent solution, it is not perfect and the accuracy of future work will depend on the tight control of this and other aspects of the SWAT Machine's operation.

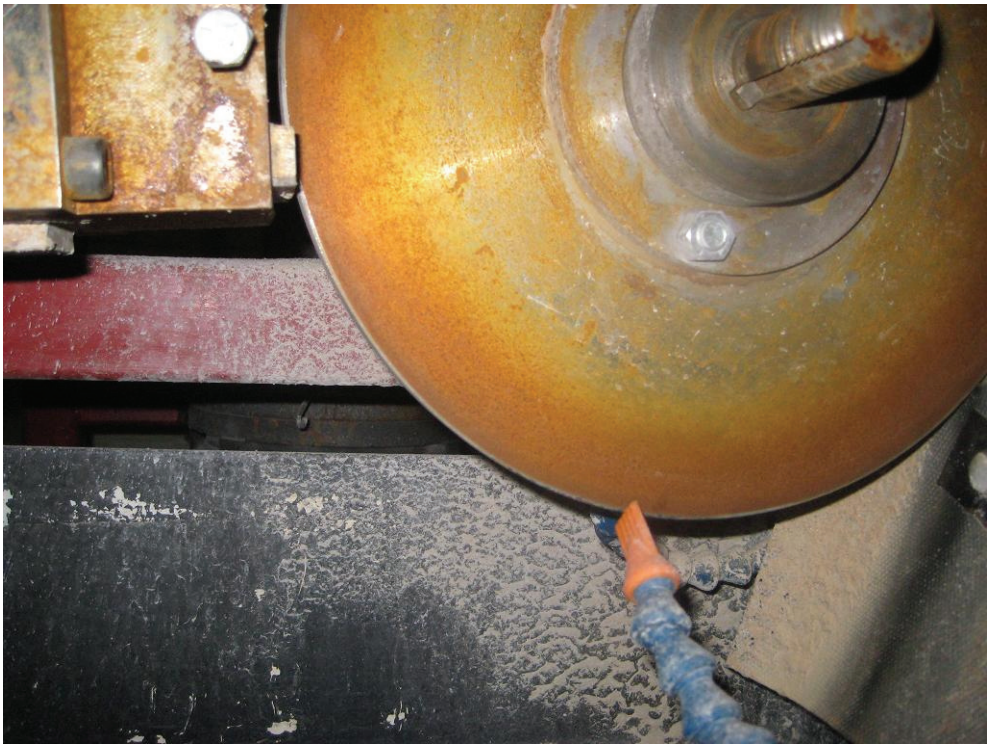

Figure 7.2: New water flushing system used for wet tests.

Having examined the breakage of standard foundry sand, the attention must now be focused on industrial ores, that is, this work must be repeated for valuable minerals extracted from the ground in order to build a database and then determine the correlation between results generated from the SWAT Machine compared to the traditional Bond Work Index methods currently used in labs and industry around the world. As ores are added to such a database, the proposed model will become more accurate. This would

mirror the success of the Total Media Wear Model. These extra tests must be complemented by more Locked-cycle tests for each of the ores tested.

Finally, future consideration should be given to further examine slurry testing. The procedure was hastily created in an effort to obtain meaningful data from an uncooperative abrasive feed. As a testament to the repeatability of the SWAT Machine, it delivered results in-line with our initial expectations, but much like wet testing, it could use more exploration and testing in order to ascertain its robustness as a credible test procedure for media wear and ore breakage.

REFERENCES

Aksani, B. and B. Sonmez (2000). "Simulation of bond grindability test by using cumulative based kinetic model." Minerals Engineering **13**(6): 673-677.

ASTM (2006). Standard Test Method for Measuring Abrasion Using the Dry Sand/Rubber Wheel Apparatus. Philadelphia, PA, ASTM International.

Binsfeld, E. "Binsfeld Engineering." Retrieved August, 2009.

Bond, F. C. (1952). "Third Theory of Comminution." Transactions of the American Institute of Mining Engineering **193**: 484-494.

Bond, F. C. (1960). "Crushing & Grinding Calculations Part 1." British Chemical Engineering **6**(6): 378-385.

Chakrabarti, D. M. (2000). "Simple approach to estimation of the work index." Transactions of the Institution of Mining and Metallurgy Section C-Mineral Processing and Extractive Metallurgy **109**: C83-C89.

Chenje, T. and P. Radziszewski (2004). Determining the steel media abrasive wear as a function of applied force and friction.

Chenje, T., P. Radziszewski, et al. (2009). Steel Media Wear: Experimentation, Simulation and Validation. 41st Annual Canadian Mineral Processors Conference, Ottawa.

Chenje, T. W. (2007). DEVELOPMENT AND VALIDATION OF A MODEL FOR STEEL GRINDING MEDIA WEAR IN TUMBLING MILLS. Department of Mechanical Engineering. Montreal, McGill University. **Doctor of Philosophy**.

Deniz, V. and H. Ozdag (2003). "A new approach to Bond grindability and work index: dynamic elastic parameters." Minerals Engineering **16**(3): 211-217.

Free, K. S., M. K. McCarter, et al. (2005). "Evaluation of a new method for work index estimation using single particle impact tests." Minerals & Metallurgical Processing **22**(2): 96-100.

Gates, J. D., G. J. Gore, et al. (2007). "The meaning of high stress abrasion and its application in white cast irons." Wear **263**(1-6): 6-35.

Hawk, J. A., R. D. Wilson, et al. (1999). Laboratory abrasive wear tests: investigation of test methods and alloy correlation.

Hewitt, D., S. Allard, et al. "Pipe lining abrasion testing for paste backfill operations." Minerals Engineering **In Press, Corrected Proof**.

Menendez-Aguado, J. M., B. R. Dzioba, et al. (2005). "Determination of work index in a common laboratory mill." Minerals & Metallurgical Processing **22**(3): 173-176.

Misra, A. and I. Finnie (1980). "A classification of three-body abrasive wear and design of a new tester." Wear **60**(1): 111-121.

Mosher, J. B. and C. B. Tague (2001). Conduct and precision of bond grindability testing.

Narayanan, S. S. (1987). "Modelling the performance of industrial ball mills using single particle breakage data." International Journal of Mineral Processing **20**(3-4): 211-228.

Powell, M. S. and R. D. Morrison (2007). "The future of comminution modelling." International Journal of Mineral Processing **84**(1-4): 228-239.

Radziszewski, P. (2002). "Exploring total media wear." Minerals Engineering **15**(12): 1073-1087.

Radziszewski, P. (2009). "The steel wheel abrasion test (SWAT): A tool to study wear, friction and ore breakage in the mining industry." Wear **267**(1-4): 92-98.
Radziszewski, P., D. Hewitt, et al. (2008). Exploring Abrasive Wear, Friction and Ore Breakage XXIV International Mineral Processing Congress, Beijing, China Scientific Book Services.
Radziszewski, P., R. Varadi, et al. (2005). "Tumbling mill steel media abrasion wear test development." Minerals Engineering **18**(3): 333-341.
Tuzun, M. A. (2001). "Wet Bond mill test." Minerals Engineering **14**(3): 369-373.

APPENDIX A

Opta Minerals Inc.

407 Parkside Drive, Waterdown, Ontario L0R 2H0
Tel: (905) 689-6661 Toll Free: (888) 689-6661 Fax: (905) 689-0485
www.optaminerals.com

TECHNICAL DATA SHEET

BARCO 32

Barco silica sands are used for a variety of foundry, steel manufacture, and industrial applications.

Typical Chemical Analysis (%):

Silicon Dioxide (total)	SiO_2	> 99.50
Titanium Oxide	TiO_2	~ 0.10
Potassium Oxide	K_2O	~ 0.10
Calcium Oxide	CaO	~ 0.03
Iron Oxide	Fe_2O_3	~ 0.03
Aluminum Oxide	Al_2O_3	~ 0.01
Loss On Ignition	LOI	~ 0.12

Typical Physical Properties:

Colour..... White
Mineral..... Quartz
Moisture..... < 0.20%
Solubility..... Insoluble
Specific Gravity (g/cc)..... 2.65
Grain Shape.....Rounded
Bulk Density..... 99 lbs./ft.^{3}
Hardness (Mohs)..... 7
Melting Point (°F).....~3100
Melting Point (°C).....~1700

Typical Gradation:

U.S. Mesh	Microns	Per Cent Retained	Per Cent Passing
20	850	0.1	99.9
30	600	9.4	90.5
40	425	59.6	30.9
50	300	28.4	2.5
70	212	2.1	0.4
100	150	0.3	0.1
140	106	0.1	0.0
200	75	0.0	0.0
270	53	0.0	0.0
PAN	0	0.0	0.0

Grain Fineness #: *32.5*
Nominal Size (mm): *0.40*
Effective Size (mm): *0.34*
Uniformity Coeffecient: *1.47*

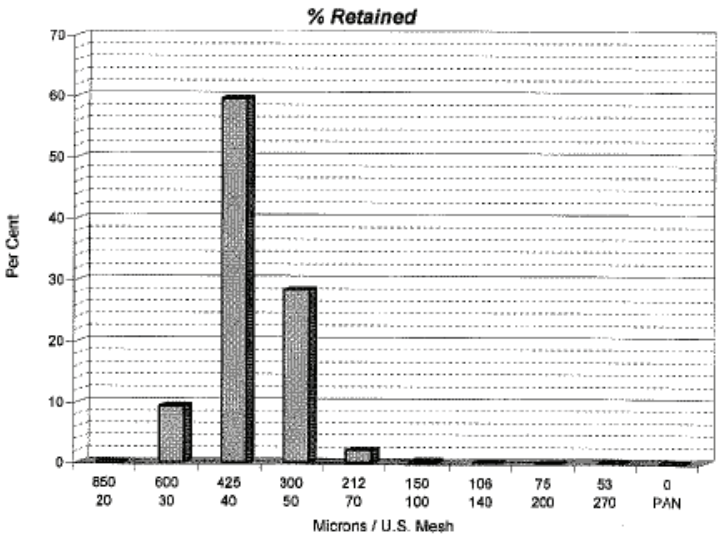

APPENDIX B

AISI 1018 Steel				
Composition		Properties		
C	0.15-0.20	Density	7.7-8.03	x1000 kg/m^3
Mn	0.60-0.92	σ_T	634	Mpa
P	0.04 Max	σ_Y	386	Mpa
S	0.05 Max	Hardness	197	HB

AISI 4140 Steel				
Composition		Properties		
C	0.38-0.43	Density	7.7-8.03	x1000 kg/m^3
Mn	0.75-1.00	σ_T	655	Mpa
P	0.035 Max	σ_Y	417	Mpa
S	0.04 Max	Hardness	197	HB*
Si	0.15-0.30			
Cr	0.80-1.10			
Mo	0.15-0.25			

*Denotes hardness at fully annealed state.

APPENDIX C

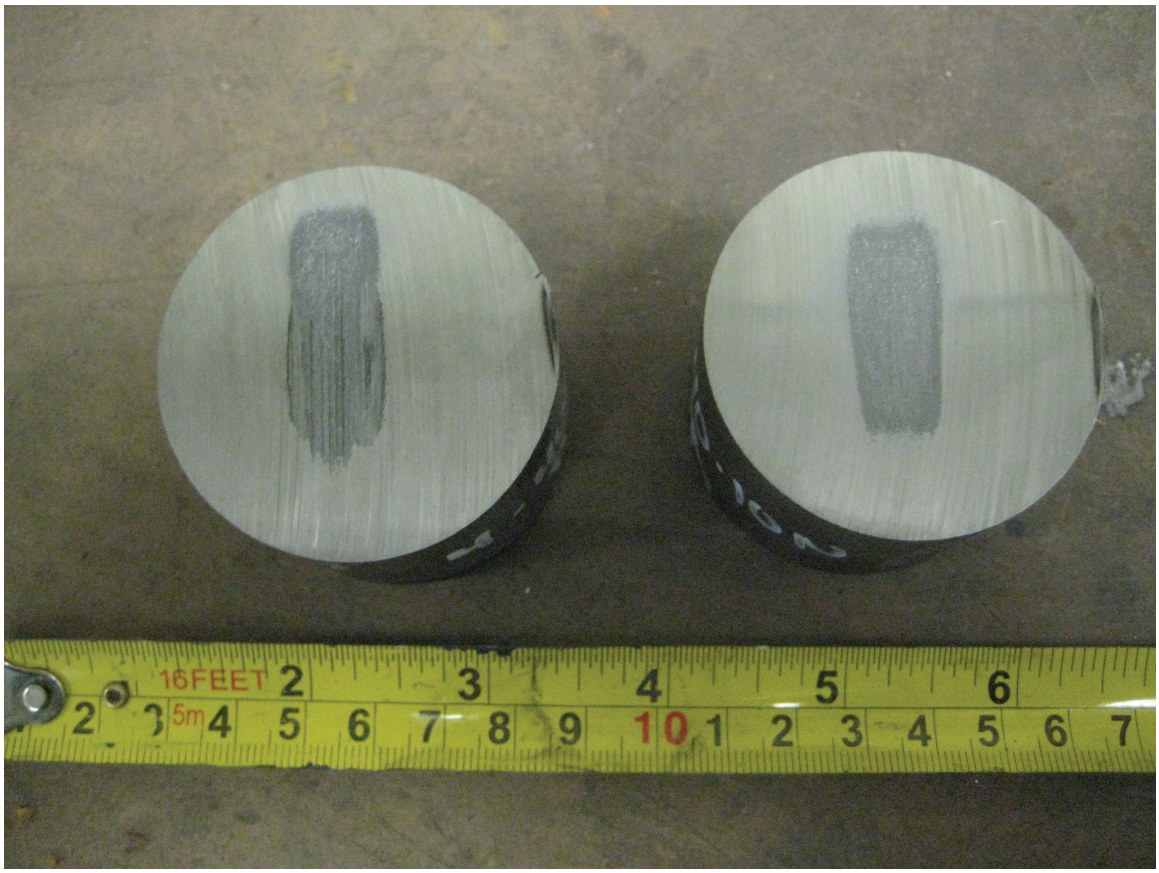

4140 Dry Test Samples showing wear scar discrepancy between high applied force (left) and low applied force (right).